NONLINEARITY OF PIEZOELECTRIC RESONATOR BASED ON $Ca_3TaGa_3Si_2O_{14}$ AND $YCa_4O(BO_3)_3$ SINGLE CRYSTALS UNDER DC BIAS FIELD

by

Xueqi Li

Bachelor of Engineering, Sichuan University, 2012

Submitted to the Graduate Faculty of

Swanson School of Engineering in partial fulfillment

of the requirements for the degree of

Master of Science

University of Pittsburgh

2018

UNIVERSITY OF PITTSBURGH

SWANSON SCHOOL OF ENGINEERING

This thesis was presented

by

Xueqi Li

It was defended on

April 2, 2018

and approved by

Qing-Ming Wang, Ph.D., Professor,

Department of Mechanical Engineering and Materials Science

Patrick Smolinski, Ph.D., Associate Professor,

Department of Mechanical Engineering and Materials Science

Williams S. Slaughter, Ph.D., Associate Professor,

Department of Mechanical Engineering and Materials Science

Thesis Advisor: Qing-Ming Wang, Ph.D., Professor,

Department of Mechanical Engineering and Materials Science

NONLINEARITY OF PIEZOELECTRIC RESONATOR BASED ON $Ca_3TaGa_3Si_2O_{14}$ AND $YCa_4O(BO_3)_3$ SINGLE CRYSTALS UNDER DC BIAS FIELD

Xueqi Li, M.S.

University of Pittsburgh, 2018

Based on the superior stability of Ca3TaGa3Si2O14 (CTGS) and $YCa_4O(BO_3)_3$ (YCOB) single crystals over a wide temperature range, this thesis work adopted Aleksandrov [1]'s method to investigate their nonlinear electromechanical properties which are crucial in the fabrication of acoustic wave devices with high-precision demand. In this research, two types of bulk acoustic wave resonators, longitudinal one and thickness shear one, have been considered separately to characterize the nonlinear permittivity, elastic coefficients as well as piezoelectric coefficients of CTGS and YCOB resonators under DC bias voltages from -180V to +180V. From the experimental results, it has been shown that resonance frequency has good linearity dependence on electric field. The nonlinear coefficients of resonators from eight crystal orientations are fully calculated, this potentially enables those two types of crystals to become frequency compensators.

In addition, a pressure tube test setup was utilized to characterize the force/pressure dependence of resonant frequency of YCOB crystal in this research. With the pressure-frequency sensitivity and nonlinear coefficients in this research, the further investigation becomes possible to explore the design and applications of high precision bulk acoustic wave pressure sensors.

TABLE OF CONTENTS

LIST OF TABLES

LIST OF FIGURES

ACKNOWLEDGEMENT

Right now, when I am finishing my master thesis, I cannot help to recall the days that I spent as a graduate student in the University of Pittsburgh which makes me a more independent and well-rounded person.

Foremost, I would like to express my deepest gratitude to my advisor, Dr. Qingming Wang who is extremely patient, thought-provoking and professional whenever I ran into a trouble or needed help with my research or career. My sincere thanks also go to my thesis committee members, Dr. William Slaughter and Dr. Patrick Smolinski for the continuous encouragement and support for my thesis.

What's more, I am also grateful to my laboratory members, Hongfei Zu and Qiuyan Li for the stimulating discussions and experience sharing. It is whole-heartedly expressed that their advice for my research is proved to be a landmark effort towards the success of my research.

I would like to pay my regards to my parents. They not only assisted me financially but also extended their support morally and emotionally through my entire life. Also, I would like to show my warm thanks to my boyfriend Wenbo Li who supported me at every bit and without whom it was impossible to accomplish the end task.

I also place on record, my sense of gratitude to one and all, who directly or indirectly, have let their hand in this venture.

1.0 INTRODUCTION

Based on the knowledge that early people obtained of tourmaline crystals, the brothers, Pierre and Jacques Curie [2], first discovered the phenomenon that mechanical load could develop polar electricity in crystals lacking inversion symmetry in 1880. One year later, Hankel [3] officially proposed the widely-accepted term “Piezoelectricity” which means “electricity caused by pressure” with “Piezo” expressing pressure in Greek. The direct piezoelectric effect is the transformation from mechanical energy into electric energy, which could be comprehended by the appearance of electric polarization when a force is exerted to the material. Most crystals processing direct piezoelectric effect will also produce a deformation when an electric field is applied, which is known as the converse piezoelectric effect. The relations of mechanical and electrical parameters are illustrated below [4]. Piezoelectricity explains the interactions between electric energy and mechanical energy.

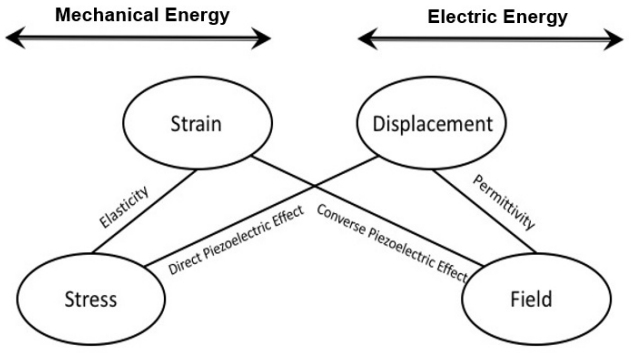

Figure 1. Relationships of mechanical quantities and electric quantities

During WW1, Langevin [5] firstly came up the idea that using piezoelectric effects to transmit and receive ultrasonic waves provides a much more effective method to detect submarines under seas. It was of obvious progressive significance in the development of echo sounding and also opened the door of ultrasonic technology which still has massive applications in modern life. Until now, a host of inventions based on both direct and converse piezoelectric effects are carried out by worldwide researchers and the applications could be easily found anywhere in our daily life. Depending on the direct piezoelectric effect, acoustic wave sensors for measuring physical quantities such as pressure, force, temperature, etc. and voltage generators have been designed and manufactured. On the other hand, converse piezoelectric effect is utilized to fabricate resonators in applications of ink printers and piezoelectric motors used in medical and micro-robotic fields. Moreover, the acoustic wave resonators are also designed as electric oscillators in feedback control loop and electric filters to obtain efficient signals [6].

1.1 HIGH TEMPERATUR PIEZOELECTRIC CRYSTALS

According to the lattice structure of crystals, there are 7 main crystal systems which are further classified by the symmetry of lattice into 32 different crystallographic point classes. Aside from 11 groups processing the feature of central symmetry and 1 class showing zero values of all piezoelectric constants due to extreme high symmetric structure, finally we get 20 crystallographic point classes potentially to be piezoelectric materials. Furthermore, each main system includes more than one classes exhibiting piezoelectricity [7, 8].

Even though crystals discovered with non-centric symmetry are beyond count, we still face the problem that only a few of them are qualified to be commercially utilized in electric device.

The requirements of piezoelectric crystals are not only restricted to high piezoelectric, dielectric and elastic constants, but also consist of stability in high temperature, absence of high hysteresis, high mechanical quality factor, etc. Several typical piezoelectric crystals which are widely accepted in commercial manufacturing will be discussed in the following.

There is no doubt that quartz (SiO_2) with outstanding characters of high mechanical quality factor, low temperature dependence under a comparatively wide temperature range and high electrical resistivity, still plays the most significant role in the application of acoustic wave sensors and oscillators in frequency standards [6]. Nevertheless, the application of quartz is restricted to the operating environment under 573℃ as phase transition from α-quartz (trigonal crystal system) to β-quartz (hexagonal crystal system) will happen when temperature grows [9]. In addition, tourmaline is another traditional representative piezoelectric crystal that has been sufficiently investigated and utilized [6, 10]. The significant drawbacks of tourmaline, high pyroelectric coefficients and difficulty in exploration for adequate quantity as well as desired quality, limits its development despite its phase change in extreme high temperature (900℃) [11, 12].

According to huge steps that has been taken in piezoelectric technology in recent decades, there are some new promising piezoelectric crystals designed, characterized and utilized. Gallium orthophosphate ($GaPO_4$), an identical quartz-like crystal, is characterized by no α-β transformation as well as good stability under 950℃, which becomes a kind of competitive material in application area under high temperature [13, 14]. In 1979, $Ca_3Ga_2Ge_4O_{14}$, which belongs to langasite family crystals started to attract people's attention with preeminent properties of no phase transformation under 1470℃ and increased sensitivity as piezoelectric sensor [15]. What's more, Rare Earth calcium oxyborate crystals have been extensively characterized to develop their application in nuclear plants and engine health motoring. This monoclinic symmetric lattice takes advantage of

high resistivity and superior electromechanical properties with low-temperature dependence until 1000℃ [6].

1.2 PHYSICAL PROPERTIES OF PIEZOELECTRIC CRYSTALS

As mentioned above, piezoelectric devices characterized by electromechanical interactions are indispensable in modern manufacturing industry. The physical properties of piezoelectric crystals which were always considered as independent components of mechanical and electric parameters should be fully investigated before large-scale production.

1.2.1 Dielectric constant

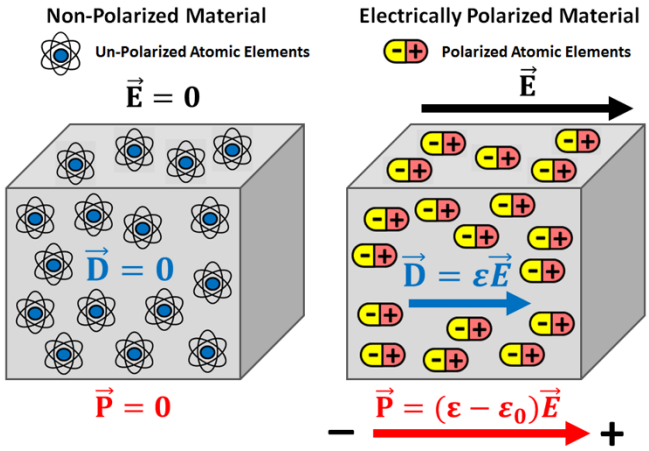

Figure 2. The atomic elements of non-polarized material and polarized material

To isotropic crystals, the orientation of electric polarization is usually the same as the direction of applied electric field. However, when it comes to piezoelectric crystals, the orientations are not limited to this specific direction because of their anisotropic characters.

The ratio of external electric field (E) and corresponding electric displacement (D) is a prime diagnosed coefficient, which is defined as dielectric permittivity (ε):

$$D_i = \varepsilon_{ij} E_j \quad where\ i,j = 1,2,3 \tag{1.2.1-1}$$

When exerting an electric field to piezoelectric crystals, the linked electric charges will be moved because of the attraction of external field to free charges [16]. P is the electric polarization density and susceptibility (χ_e) shows the extent of atoms separation on the surface under electrodes.

$$P = (\varepsilon - \varepsilon_0)E = \varepsilon_0 \chi_e E \tag{1.2.1-2}$$

In this paper, we use relative permittivity (ε_r) which is commonly accepted to express the dielectric properties compared to crystals of free-space to illustrate permittivity [17].

$$\varepsilon_r = \frac{\varepsilon}{\varepsilon_0} \tag{1.2.1-3}$$

$$\varepsilon_0 = \frac{1}{36\pi} \times 10^{-9} F/m \tag{1.2.1-4}$$

1.2.2 Elastic constant

To express the loading within a material caused by an external force and its corresponsive deformation, we use following second order tensors which are all diagnosed symmetry based on condition of static equilibrium. These matrixes could be further simplified by the principle: 11→1, 22→2, 33→3, 23→4, 13→5 and 12→6.

$$\boldsymbol{T} = \begin{bmatrix} T_{11} & T_{12} & T_{13} \\ T_{21} & T_{22} & T_{23} \\ T_{31} & T_{32} & T_{33} \end{bmatrix} = \begin{bmatrix} T_1 & T_6 & T_5 \\ T_6 & T_2 & T_4 \\ T_5 & T_4 & T_3 \end{bmatrix} \tag{1.2.2-1}$$

$$\boldsymbol{S} = \begin{bmatrix} S_{11} & S_{12} & S_{13} \\ S_{21} & S_{22} & S_{23} \\ S_{31} & S_{32} & S_{33} \end{bmatrix} = \begin{bmatrix} S_1 & \frac{S_6}{2} & \frac{S_5}{2} \\ \frac{S_6}{2} & S_2 & \frac{S_4}{2} \\ \frac{S_5}{2} & \frac{S_4}{2} & S_3 \end{bmatrix} \quad (1.2.2\text{-}2)$$

According to Generalized Hooke's Law that the stresses are proportional to the strains in the condition of small displacements, following relationships for anisotropic materials could be developed as

$$T_i = c_{ij} S_j, \qquad i, j = 1,2, \dots ,6 \quad (1.2.2\text{-}3)$$

$$S_j = s_{ij} T_i, \qquad i, j = 1,2, \dots ,6 \quad (1.2.2\text{-}4)$$

$$c_{ij} = c_{ji}, \qquad s_{ij} = s_{ji} \quad (1.2.2\text{-}5)$$

where c_{ij} and s_{ij} are elastic stiffness and compliance [18].

1.2.3 Piezoelectric constant

There are two piezoelectric constants, e_{ip} and h_{ip}, characterizing the electric field and displacement generated by mechanical stress or strain. On the contrary, the other two coefficients, g_{ip} and d_{ip} accounted for the transformation from mechanical energy to electric energy by converse piezoelectric effect.

For the denotation of piezoelectric coefficients, first subscript indicates the direction of electric parameters and the next one is related with mechanical quantities such as the internal stress produced by an external load. The definition expressions listed below are composed of another subscript outside brackets which expounds the boundary conditions [8, 19, 20]. For instance, T denotes the environment of constant stress or, alternatively, there is no mechanical load applied. The open-circuited condition or zero electric displacement is expressed by E.

There are two definition ways for piezoelectric constants. As the second terms in (1.2.3-1), converse piezoelectric effects are adopted to determine linear piezoelectric coefficients while the last terms are dependent on direct piezoelectric effects. All these 3×6 piezoelectric matrixes consist of four categories of constitutive equations which would be further discussed in the following section.

$$\begin{cases} d_{pq} = \left(\dfrac{\partial S_q}{\partial E_p}\right)_T = \left(\dfrac{\partial D_p}{\partial T_q}\right)_E \\ g_{pq} = \left(\dfrac{\partial S_q}{\partial D_p}\right)_T = -\left(\dfrac{\partial E_p}{\partial T_q}\right)_D \\ h_{pq} = -\left(\dfrac{\partial T_q}{\partial D_p}\right)_S = -\left(\dfrac{\partial E_p}{\partial S_q}\right)_D \\ e_{pq} = -\left(\dfrac{\partial T_q}{\partial E_p}\right)_S = \left(\dfrac{\partial D_p}{\partial S_q}\right)_E \end{cases} \quad (1.2.3\text{-}1)$$

1.2.4 Piezoelectric constitutive equations

Piezoelectric constitutive equations describe the relationship between mechanical quantities (stress T and strain S) and electric quantities (electric intensity E and electric displacement D) of crystals.

The derivation of these fundamental equations begins with selecting one independent variable from each pair of quantities, (E, D) and (T, S) so that there are four types of constitutive equations in total. Then appropriate state functions such as internal energy (U) are adopted to gain the final four types of constitutive equations according to Maxwell's equations. The $d-type$ equations are always introduced in crystals with longitudinal vibration while thickness shear crystals usually take e-type formulas as priority consideration to carry out further calculations [8, 20].

$$d-type\begin{cases}S_p = s_{pq}^E T_q + d_{jp}E_j \\ D_i = d_{iq}T_q + \varepsilon_{ij}^T E_j\end{cases} \quad (1.2.4\text{-}1)$$

$$g-type\begin{cases}S_p = s_{pq}^D T_q + g_{jp}D_j \\ E_i = -g_{iq}T_q + \beta_{ij}^T D_j\end{cases} \quad (1.2.4\text{-}2)$$

$$h-type\begin{cases}T_p = c_{pq}^D S_q - h_{jp}D_j \\ E_i = -h_{iq}S_q + \beta_{ij}^S D_j\end{cases} \quad (1.2.4\text{-}3)$$

$$e-type\begin{cases}T_p = c_{pq}^E S_q - e_{jp}E_j \\ D_i = e_{iq}S_q + \varepsilon_{ij}^S E_j\end{cases} \quad (1.2.4\text{-}4)$$

where $p, q = 1,2,\cdots 6$ and $i, j = 1,2,3$.

1.3 NONLINEAR EFFECTS IN PIEZOELECTRIC CRYSTALS

1.3.1 Nonlinear effects

The linear coefficients of piezoelectric crystals such as quartz have already been investigated extensively and widely applied in modern manufacturing industry [6, 18, 19]. Nevertheless, when applied to some higher driving levels, the occurrence of distortions and harmonic frequency in the response figure reminds people the existence of nonlinear effects which would prevent the applications as accurate electric devices [20]. Hence, it is an insistent demand to carry out investigations on nonlinear electromechanical properties.

The origins of those nonlinear effects appearing under the environment of high oscillation level are sophisticated, which could be summarized in two aspects, geometrical nonlinearities and material nonlinearities [17]. One identical nonlinear electromechanical property is electrostrictive coefficient relating the strain and second order of electric field or polarization shown in a large

variety of crystals and ceramics [21, 22]. Beyond that, nonlinear permittivity and piezoelectric coefficients should also be characterized to promote understanding on nonlinear behavior of crystals. Nonlinear effects not only could be utilized in the manufacturing of correlators for microwave acoustic devices [23], but also have potential in temperature-frequency controller. For instance, the frequency shifts caused by the alteration of temperature in the sensitive temperature sensor could be compensated through an added direct current (DC) bias field [24].

Until now, the research achievement on nonlinear properties are limited. One effective way to characterize nonlinear elastic constants is based on the force-frequency effect by adding an external load according to Lee [25]'s deviation. In addition, it has been noticed that a DC bias field could lead to frequency shift in piezoelectric resonator probably by changing the geometric dimensions as well as elastic coefficients as a result of nonlinear properties [24, 26, 27]. DC bias as a strong electric field could weaken the effect of residual stresses and then enhance the effective coefficients. Aleksandrov et al.[1] derived another utilization for the DC bias field, which is considered to characterize nonlinear modulus of single crystal resonators by taking effective coefficients composed of nonlinear constants and corresponding DC bias field.

1.3.2 Nonlinear piezoelectric constitutive equations

Depending on the assumption of linear piezoelectric effect, constitutive equations has been deduced and summarized. When studying the nonlinear connections between those electromechanical coefficients, J. Gagnepain and R. Besson [20] worked out advanced "piezoelectric eqautions" by including higher order terms with regard to independent viarables in linear functions. This form has been generally adopted within investigation and calculation in

nonlinear piezoelectricity [21, 28]. The nonlinear expressions for d-type equations are demonstrated in the following equations.

$$S_i = s_{ij}T_j + \frac{1}{2}s_{ijk}T_jT_k + \frac{1}{6}s_{ijkl}T_jT_kT_l + \cdots + d_{mi}E_m + \frac{1}{2}d_{mn,i}E_mE_n + d_{m,ij}E_mT_j + \frac{1}{2}d_{m,ijk}E_mT_jT_k + \frac{1}{2}d_{mn,ij}E_mE_nT_j + \frac{1}{6}d_{mnp,i}E_mE_nE_p + \cdots \quad (1.3.2\text{-}1)$$

$$D_h = d_{hj}T_j + d_{hm,j}E_mT_j + \frac{1}{2}d_{h,jk}T_jT_k + \frac{1}{6}d_{h,jkl}T_jT_kT_l + \frac{1}{2}d_{hm,jk}E_mT_jT_k + \frac{1}{2}d_{hmn,j}E_mE_nT_j + \cdots + \varepsilon_{hm}E_m + \frac{1}{2}\varepsilon_{hmn}E_mE_n + \frac{1}{6}\varepsilon_{hmnp}E_mE_nE_p + \cdots \quad (1.3.2\text{-}2)$$

s_{ij}, s_{ijk} and s_{ijkl} are the elastic coefficients of second, third and fourth order respectively while ε_{hm}, ε_{hm} and ε_{hmnp} are the corresponding permittivity. It is worth noticing that there is a comma among the notation in subscript dividing electric quantities on the left side to strains or stresses on the other side. What's more, such properties should also be taken care of according to the derivation process of nonlinear coefficients [20].

$$d_{hm,j} = d_{mh,j} \text{ and } d_{h,jkl} = d_{h,kjl} = d_{h,jkl} \quad (1.3.2\text{-}3)$$

$$\text{but } d_{hm,j} \neq d_{m,hj} \text{ and } d_{h,jkl} \neq d_{hk,jl} \neq d_{hjk,l} \quad (1.3.2\text{-}4)$$

1.4 MOTIVATION

With the promoting and intensive development of piezoelectric devices, it is an imminent demand to seek out a new piezoelectric crystal which is still processing good stability under high temperature environment, and whose nonlinear properties should be characterized for purpose of practical applications with more accurate requirement. As mentioned above, the langasite family crystals and calcium oxyborate crystals with rare earth elements are two ascendant types of piezoelectric materials outstanding for superior electromechanical properties such as high electric resistivity and low temperature dependent. Therefore, we choose $Ca_3TaGa_3Si_2O_4$ (CTGS) crystals and $YCa_4O(BO_3)_3$ (YCOB) crystals from these two catalogues respectively to carry out the investigation of nonlinear properties. The method firstly raised by Aleksandrov et al. [1] would be employed to calculating nonlinear elastic coefficients, permittivity and electrostrictive constants under a DC bias field. What's more, the sensitivity of some YCOB pressure sensors has been tested which develops more possibilities for this Rare Earth calcium oxyborate crystal.

2.0 THEORETICAL ANALYSIS

The calculation method for nonlinear piezoelectric properties is undoubtedly significant not only for better comprehend nonlinear electromechanical effects, but also for utilization in design as well as manufacturing of electric devices with more precise requirements. In this chapter, the basic parameters of single piezoelectric crystals adopted in this research will be illustrated first. Besides, the theoretical method that we propose to determine nonlinear coefficients will be fully explained later.

2.1 GENERAL INFORMATION OF CTGS AND YCOB CRYSTALS

2.1.1 CTGS crystals

$Ca_3TaGa_3Si_2O_{14}$ (CTGS), classified as a 32 points trigonal crystal, is a representative piezoelectric fully ordered single crystal with excellent stability and high temperature behaviors whose linear coefficients have been sufficiently measured [29, 30]. As a result, we choose CTGS as one of potential piezoelectric materials to experiment with.

As mentioned before, the symmetricity of crystal lattice categorizes all crystals into 32 classes. Because of the feature that symmetric structure is based on threefold axis, the independent linear electromechanical coefficients owned by CTGS crystals reduce dramatically.

For permittivity, CTGS crystals have only 2 dependent constants, ε_{11} and ε_{33} which bring diagonal symmetry to dielectric matrix.

$$\varepsilon_{pq} = \begin{bmatrix} \varepsilon_{11} & 0 & 0 \\ 0 & \varepsilon_{11} & 0 \\ 0 & 0 & \varepsilon_{33} \end{bmatrix} \quad (2.1.1\text{-}1)$$

$$\beta_{pq} = \begin{bmatrix} \beta_{11} & 0 & 0 \\ 0 & \beta_{11} & 0 \\ 0 & 0 & \beta_{33} \end{bmatrix} \quad (2.1.1\text{-}2)$$

$$\varepsilon_{pq} = {\beta_{pq}}^{-1} \quad (2.1.1\text{-}3)$$

It can be seen from the following expressions that each matrix of elastic compliance and stiffness contains 6 independent components and are linearly inverse from each other.

$$s_{pq} = \begin{bmatrix} s_{11} & s_{12} & s_{13} & s_{14} & 0 & 0 \\ s_{12} & s_{11} & s_{13} & -s_{14} & 0 & 0 \\ s_{13} & s_{13} & s_{33} & 0 & 0 & 0 \\ s_{14} & -s_{14} & 0 & s_{44} & 0 & 0 \\ 0 & 0 & 0 & 0 & s_{44} & 2s_{14} \\ 0 & 0 & 0 & 0 & s_{14} & 2(s_{11} - s_{12}) \end{bmatrix} \quad (2.1.1\text{-}4)$$

$$c_{pq} = \begin{bmatrix} c_{11} & c_{12} & c_{13} & c_{14} & 0 & 0 \\ c_{12} & c_{11} & c_{13} & -c_{14} & 0 & 0 \\ c_{13} & c_{13} & c_{33} & 0 & 0 & 0 \\ c_{14} & -c_{14} & 0 & c_{44} & 0 & 0 \\ 0 & 0 & 0 & 0 & c_{44} & 2c_{14} \\ 0 & 0 & 0 & 0 & c_{14} & \dfrac{c_{11} - c_{12}}{2} \end{bmatrix} \quad (2.1.1\text{-}5)$$

$$c_{pq} = {s_{pq}}^{-1} \quad (2.1.1\text{-}6)$$

Trigonal crystals in point group 32 only have 2 independent piezoelectric constants. Two matrices of CTGS are shown below, these matrices will be adopted for the calculation later.

$$d_{pq} = \begin{bmatrix} d_{11} & -d_{11} & 0 & d_{14} & 0 & 0 \\ 0 & 0 & 0 & 0 & -d_{14} & -2d_{11} \\ 0 & 0 & 0 & 0 & 0 & 0 \end{bmatrix} \quad (2.1.1\text{-}7)$$

$$e_{pq} = \begin{bmatrix} e_{11} & -e_{11} & 0 & e_{14} & 0 & 0 \\ 0 & 0 & 0 & 0 & -e_{14} & -2e_{11} \\ 0 & 0 & 0 & 0 & 0 & 0 \end{bmatrix} \quad (2.1.1\text{-}8)$$

$$e_{ip} = d_{iq} c_{qp}^{E} \quad (2.1.1\text{-}9)$$

2.1.2 YCOB crystals

In addition to the langasite family crystals, calcium oxyborate crystals with rare earth elements are outstanding for their extremely high transition temperature (1500 ℃) and also excellent permittivity and piezoelectricity compared to other materials. The singe yttrium calcium oxyborate crystal $YCa_4O(BO_3)_3$ abbreviated as YCOB, are standing out from other Rare Earth crystals because of their preferable electromechanical properties and relatively simplicity in production.

Compared to the corresponding features of CTGS crystals, YCOB crystals have more complicated matrices and much more independent linear coefficients because of the various classes they belong to. The tensors of permittivity, elastic compliance and piezoelectric coefficients are illustrated below respectively. Other YCOB parameters have same relationships as that of CTGS.

$$\varepsilon_{pq} = \begin{bmatrix} \varepsilon_{11} & 0 & \varepsilon_{13} \\ 0 & \varepsilon_{22} & 0 \\ \varepsilon_{13} & 0 & \varepsilon_{33} \end{bmatrix} \quad (2.1.2\text{-}1)$$

$$d_{pq} = \begin{bmatrix} d_{11} & d_{12} & d_{13} & 0 & d_{15} & 0 \\ 0 & 0 & 0 & d_{24} & 0 & d_{26} \\ d_{31} & d_{32} & d_{33} & 0 & d_{35} & 0 \end{bmatrix} \quad (2.1.2\text{-}2)$$

$$s_{pq} = \begin{bmatrix} s_{11} & s_{12} & s_{13} & 0 & s_{15} & 0 \\ s_{12} & s_{22} & s_{23} & 0 & s_{25} & 0 \\ s_{13} & s_{23} & s_{33} & 0 & s_{35} & 0 \\ 0 & 0 & 0 & s_{44} & 0 & s_{46} \\ s_{15} & s_{25} & s_{35} & 0 & s_{55} & 0 \\ 0 & 0 & 0 & s_{46} & 0 & s_{66} \end{bmatrix} \quad (2.1.2\text{-}3)$$

2.2 DETERMINATION OF NONLINEAR COEFFICIENTS BY APPYING A DC BIAS FIELD

Although the method to determine linear coefficients has been extensively illustrated [8], there is only a few investigations upon nonlinear effects which is crucial to precise applications of electric devices. Here we adopt ALEKSANDROV [1]'s approach that applying a DC bias field to excite longitudinal and thickness shear vibrations of piezoelectric resonators. Then the nonlinear parameters can be worked out based on linear deductive method.

2.2.1 Piezoelectric resonators with longitudinal vibration

For piezoelectric resonators with longitudinal vibration, electrodes are deposited on the surface normal to the direction of thickness. General forms for linear constitutive equations are

$$S_p = s_{pq}^E T_q + d_{jp} E_j \quad (2.2.1\text{-}1)$$

$$D_i = d_{iq} T_q + \varepsilon_{ij}^T E_j \quad (2.2.1\text{-}2)$$

Considering nonlinear terms expanded by variables **T** and **E**, we could obtain nonlinear expressions

$$S_p = s_{pq}^E T_q + d_{jp} E_j + \frac{1}{2} s_{pqq}^E {T_q}^2 + \frac{1}{2} M_{jp} {E_j}^2 + d_{jpq}^{\mathrm{E}} E_j T_q \quad (2.2.1\text{-}3)$$

$$D_i = d_{iq} T_q + \varepsilon_{ij}^T E_j + \frac{1}{2} d_{iqq}^{\mathrm{E}} {T_q}^2 + \frac{1}{2} \varepsilon_{ijj}^T {E_j}^2 + M_{jq} E_j T_q \quad (2.2.1\text{-}4)$$

where s_{pqq}^E , d_{jpq} , ε_{ijj}^T and M_{jp} are nonlinear elastic compliance, piezoelectric constant, permittivity and electrostrictive constant.

If we assume that both a direct current and a small alternating current are applied to resonators, most electromechanical variables would be written in the combination of a static term

and a dynamic term except strain. There is no static segment for strain in the condition that electric field is the only nonzero electromechanical quantity.

$$E_j = \bar{E}_j + \tilde{E}_j \quad (2.2.1\text{-}5)$$

$$S_p = \bar{S}_p + \tilde{S}_p \quad (2.2.1\text{-}6)$$

$$D_i = \bar{D}_i + \tilde{D}_i \quad (2.2.1\text{-}7)$$

$$T_q = \tilde{T}_q \quad (2.2.1\text{-}8)$$

Firstly, by substituting above combinations to nonlinear constitutive equations, we have three variables, $\bar{E}_j$, $\tilde{E}_j$and $\tilde{T}_q$ instead of two original parameters, E and T. The second step is to refine expressions by taking first-order approximation and then leave dynamic parts:

$$\tilde{S}_p = s_{pq}^E \tilde{T}_q + d_{jp}\tilde{E}_j + M_{jp}\bar{E}_j\tilde{E}_j + d_{jpq}^{\mathrm{E}}\bar{E}_j\tilde{T}_q \quad (2.2.1\text{-}9)$$

$$\tilde{D}_i = d_{iq}\tilde{T}_q + \varepsilon_{ij}^T\tilde{E}_j + \varepsilon_{ijj}^T\bar{E}_j\tilde{E}_j + M_{jq}\bar{E}_j\tilde{T}_q \quad (2.2.1\text{-}10)$$

Afterwards, the nonlinear equations are reformulated in linear forms by introducing effective constants which are dependent on the DC bias field. The effective constants consist of corresponding linear constants, the product of nonlinear constants and the DC bias field.

$$\tilde{S}_p = s_{pq}^{\mathrm{eff}}\tilde{T}_q + d_{jp}^{\mathrm{eff}}\tilde{E}_j \quad (2.2.1\text{-}11)$$

$$\tilde{D}_i = d_{iq}^{\mathrm{eff}}\tilde{T}_q + \varepsilon_{ij}^{\mathrm{eff}}\tilde{E}_j \quad (2.2.1\text{-}12)$$

where

$$s_{pq}^{\mathrm{eff}} = s_{pq}^{\mathrm{E}}\left(1 + \frac{d_{jpq}^{\mathrm{E}}}{s_{pq}^{\mathrm{E}}}\bar{E}_j\right) \quad (2.2.1\text{-}13)$$

$$d_{jp}^{\mathrm{eff}} = d_{jp}\left(1 + \frac{M_{jq}}{d_{jp}}\bar{E}_j\right) \quad (2.2.1\text{-}14)$$

$$\varepsilon_{ij}^{\mathrm{eff}} = \varepsilon_{ij}^{\mathrm{T}}\left(1 + \frac{\varepsilon_{ijj}^{\mathrm{T}}}{\varepsilon_{ij}^{\mathrm{T}}}\bar{E}_j\right) \quad (2.2.1\text{-}15)$$

It is discovered that nonlinear constants could be easily characterized by evaluating effective constants from IEEE method because of their linear connections with each other. Considering the different types of constant matrices mentioned above, nonlinear properties of one CTGS resonator (XY-cut) and three YCOB resonators (XY-cut, ZX-cut and ZY-cut) could be measured with this method. The specific steps to evaluate nonlinear parameters are illustrated below by taking XY-cut CTGS resonator as an example, whose thickness and longitudinal directions are along X axis and Y axis, respectively.

As the electric field is located on the top and bottom surfaces, the resonator will be polarized along the orientation of thickness which leads to

$$E_1 \neq 0 \text{ and } E_2 = E_3 = 0 \quad (2.2.1\text{-}16)$$

In addition to the two surfaces normal to its longitudinal direction, all other faces are assumed to be free. Then we could obtain another boundary condition:

$$T_2 \neq 0 \text{ and } T_1 = T_3 = T_4 = T_5 = T_6 = 0 \quad (2.2.1\text{-}17)$$

In this case, d-type constitutive equations are accepted to simplify the process of analysis:

$$\tilde{S}_2 = s_{22}^{\text{eff}}\tilde{T}_2 + d_{12}^{\text{eff}}\tilde{E}_1 \quad (2.2.1\text{-}18)$$

$$\widetilde{D}_1 = d_{12}^{\text{eff}}\tilde{T}_2 + \varepsilon_{11}^{\text{eff}}\tilde{E}_1 \quad (2.2.1\text{-}19)$$

where

$$s_{22}^{\text{eff}} = s_{22}^{\text{E}}\left(1 + \frac{d_{122}^{\text{E}}}{s_{22}^{\text{E}}}\bar{E}_1\right) \quad (2.2.1\text{-}20)$$

$$d_{12}^{\text{eff}} = d_{12}\left(1 + \frac{M_{12}}{d_{12}}\bar{E}_1\right) \quad (2.2.1\text{-}21)$$

$$\varepsilon_{11}^{\text{eff}} = \varepsilon_{11}^{\text{T}}\left(1 + \frac{\varepsilon_{111}^{\text{T}}}{\varepsilon_{11}^{\text{T}}}\bar{E}_1\right) \quad (2.2.1\text{-}22)$$

Since the only nonzero stress is T_2, the equation of motion for this longitudinal vibration resonator is

$$\rho \frac{\partial^2 u}{\partial t^2} = \frac{\partial T_2}{\partial y} \quad (2.2.1\text{-}23)$$

By substituting constitutive equations and boundary conditions, the equation of motion becomes

$$\rho \frac{\partial^2 u}{\partial t^2} = \frac{1}{s_{22}^{\text{eff}}} \frac{\partial^2 u_2}{\partial y^2} \quad (2.2.1\text{-}24)$$

As the solution is given in the form of $u_1 = ue^{jwt}$, the effective elastic compliance based on the DC bias field has following relationship with acoustic wave velocity in Y direction:

$$v = \sqrt{\frac{1}{\rho s_{22}^{\text{eff}}}} \quad (2.2.1\text{-}25)$$

After that, the expression for admittance is deduced based on circuit state equations and vibration equations:

$$Y = j\omega \frac{\varepsilon_{11}^{\text{eff}} w^{\text{eff}} l^{\text{eff}}}{t^{\text{eff}}} \left[\left(1 - (k_{12}^{\text{eff}})^2\right) + (k_{12}^{\text{eff}})^2 \frac{\tan(\frac{kl^{\text{eff}}}{2})}{\frac{kl^{\text{eff}}}{2}} \right] \quad (2.2.1\text{-}26)$$

$$k = \frac{\omega}{v} \quad (2.2.1\text{-}27)$$

where t^{eff} and k_{12} are effective thickness and electromechanical coupling factor while l^{eff} and w^{eff} are the effective length and width covered by electrode under a DC bias field.

2.2.1.1 Nonlinear permittivity

According to IEEE standard, linear permittivity should be characterized from capacitance of corresponding orientation as well as three dimensions. Here, we could evaluate nonlinear dielectric coefficients from effective permittivity by the means of taking effective permittivity as linear

properties made up of third order coefficients and electric field. What's more, the application of the DC bias field will directly cause the deformation of resonator that we should also pay attention to:

$$t^{\text{eff}} = (1 + d_{11}\bar{E}_1)t \quad (2.2.1\text{-}28)$$

$$l^{\text{eff}} = (1 - d_{11}\bar{E}_1)l \quad (2.2.1\text{-}29)$$

$$w^{\text{eff}} = w \quad (2.2.1\text{-}30)$$

where t is thickness while l and w are the length and width covered by electrode without electric field. In the condition of low frequency,

$$\frac{\tan(\frac{kl^{\text{eff}}}{2})}{\frac{kl^{\text{eff}}}{2}} \to 1 \quad (2.2.1\text{-}31)$$

Thus, the effective permittivity measured at constant stress is gained by $Y^T = j\omega C^T$ that

$$\varepsilon_{11}^{\text{eff}} = \frac{C^T t^{\text{eff}}}{w^{\text{eff}} l^{\text{eff}}} = \frac{C^T t(1 + d_{11}\bar{E}_1)}{wl(1 - d_{11}\bar{E}_1)} \quad (2.2.1\text{-}32)$$

where C^T is the capacitance obtained at low frequency(1kHz). Taking Eq. (2.2.1-22) into consideration, we finally come to the expression for nonlinear permittivity:

$$\varepsilon_{111}^{\text{T}} = \frac{\varepsilon_{11}^{\text{eff}} - \varepsilon_{11}^{\text{T}}}{\bar{E}_1} \quad (2.2.1\text{-}33)$$

2.2.1.2 Nonlinear piezoelectric constant

When $Y \to \infty$,

$$tan\left(\frac{kl^{\text{eff}}}{2}\right) = tan\left(\frac{\omega l^{\text{eff}}}{2v}\right) \to \infty \quad (2.2.1\text{-}34)$$

The resonance frequency (f_r) is denoted as

$$f_r = \frac{v}{2l^{\text{eff}}} = \frac{1}{2l^{\text{eff}}\sqrt{\rho s_{22}^{\text{eff}}}} \quad (2.2.1\text{-}35)$$

In other words,

$$s_{22}^{\text{eff}} = \frac{1}{4\rho(l^{\text{eff}} f_r)^2} \quad (2.2.1\text{-}36)$$

where ρ represents the density of resonator. It could be evaluated from the definition of s_{22}^{eff} that nonlinear piezoelectric coefficient under constant electric field is

$$d_{122}^{\text{E}} = \frac{s_{22}^{\text{eff}} - s_{22}^{\text{E}}}{\bar{E}_1} \quad (2.2.1\text{-}37)$$

2.2.1.3 Electrostrictive constant

From the two effective coefficients (s_{22}^{eff} and $\varepsilon_{11}^{\text{eff}}$), another nonlinear parameter, electrostrictive constant, could be measured by following relationship:

$$d_{12}^{\text{eff}} = k_{12}^{\text{eff}}\sqrt{\varepsilon_{11}^{\text{eff}} s_{22}^{\text{eff}}} \quad (2.2.1\text{-}38)$$

where electromechanical coupling factor k_{31}^{eff} is derived when $Y \to 0$,

$$\frac{(k_{12}^{\text{eff}})^2 - 1}{(k_{12}^{\text{eff}})^2} = \frac{\tan\left[\frac{\pi}{2}\left(\frac{f_a}{f_r}\right)\right]}{\frac{\pi}{2}\left(\frac{f_a}{f_r}\right)} \quad (2.2.1\text{-}39)$$

where f_a is the anti-resonance frequency of resonator. Therefore,

$$\mathrm{M}_{12} = \frac{d_{12}^{\text{eff}} - d_{12}}{\bar{E}_1} \quad (2.2.1\text{-}40)$$

is the function to determine nonlinear electrostrictive coefficient.

2.2.2 Piezoelectric resonators with thickness shear vibration

Apart from longitudinal vibration mode, another identical mode is also employed to evaluate more nonlinear properties, which is thickness shear vibration. For this kind of resonators, vibration along thickness direction is the dominant motion.

To reduce the difficulty during calculation, we usually choose e-type linear constitutive equations:

$$T_p = c_{pq}^E S_q - e_{jp} E_j \quad (2.2.2\text{-}1)$$

$$D_i = e_{iq} S_q + \varepsilon_{ij}^S E_j \quad (2.2.2\text{-}2)$$

Then similar steps are taken to characterize nonlinear coefficients of crystals vibrated in the orientation of thickness. Nonlinear constitutive equations are firstly developed depending on strain and electric displacement.

$$T_p = c_{pq}^E S_q - e_{jp} E_j + \frac{1}{2} c_{pqq}^E {S_q}^2 - \frac{1}{2} M_{jp} {E_j}^2 - \mathrm{e}_{jpg}^E E_j S_q \quad (2.2.2\text{-}3)$$

$$D_i = e_{iq} S_q + \varepsilon_{ij}^S E_j + \frac{1}{2} \mathrm{e}_{iqq}^E {S_q}^2 + \frac{1}{2} \varepsilon_{ijj}^S {E_j}^2 + M_{jq} E_j S_q \quad (2.2.2\text{-}4)$$

where c_{pqq}^E , e_{jpg}^E , ε_{ijj}^S and M_{jp} are the nonlinear elastic stiffness, piezoelectric constant, permittivity and electrostrictive constant respectively.

Secondly, electromechanical variables are divided into static and dynamic parts and then the principle of first approximation are followed to refine above equations.

$$E_j = \bar{E}_j + \tilde{E}_j \quad (2.2.2\text{-}5)$$

$$T_p = \bar{T}_p + \tilde{T}_p \quad (2.2.2\text{-}6)$$

$$D_i = \bar{D}_i + \tilde{D}_i \quad (2.2.2\text{-}7)$$

$$S_q = \tilde{S}_q \quad (2.2.2\text{-}8)$$

$$\tilde{T}_p = c_{pq}^{\text{eff}} \tilde{S}_q - e_{jp}^{\text{eff}} \tilde{E}_j \quad (2.2.2\text{-}9)$$

$$\tilde{D}_i = e_{iq}^{\text{eff}} \tilde{S}_q + \varepsilon_{ij}^{\text{eff}} \tilde{E}_j \quad (2.2.2\text{-}10)$$

where

$$c_{pq}^{\text{eff}} = c_{pq}^{\text{E}} \left(1 - \frac{e_{jpq}^{\text{E}}}{c_{pq}^{\text{E}}} \bar{E}_j \right) \quad (2.2.2\text{-}11)$$

$$e_{jp}^{\text{eff}} = e_{jp} \left(1 + \frac{M_{jq}}{e_{jp}} \bar{E}_j \right) \quad (2.2.2\text{-}12)$$

$$\varepsilon_{ij}^{\text{eff}} = \varepsilon_{ij}^{\text{S}} \left(1 + \frac{\varepsilon_{ijj}^{\text{S}}}{\varepsilon_{ij}^{\text{S}}} \bar{E}_j \right) \quad (2.2.2\text{-}13)$$

Dependent on the symmetry and quantities of piezoelectric constants, we could only find one cut (Y-cut) of CTGS crystals that efficiently carries out further investigation. However, for YCOB crystals, all three cuts whose thickness is along X, Y and Z axis are appropriate for this approach. Here, we will select X-cut of YCOB crystal to explain derivation process.

The resonator is polarized along its thickness direction (along X axis), then

$$D_1 \neq 0 \text{ and } D_2 = D_3 = 0 \quad (2.2.2\text{-}14)$$

and the force is only applied on the faces with electrodes, thus

$$S_5 \neq 0 \text{ and } S_1 = S_2 = S_3 = S_4 = S_6 = 0 \quad (2.2.2\text{-}15)$$

The e-type constitutive equations with effective constants are

$$\tilde{T}_5 = c_{55}^{\text{eff}} \tilde{S}_5 - e_{15}^{\text{eff}} \tilde{E}_1 \quad (2.2.2\text{-}16)$$

$$\tilde{D}_1 = e_{15}^{\text{eff}} \tilde{S}_5 + \varepsilon_{11}^{\text{eff}} \tilde{E}_1 \quad (2.2.2\text{-}17)$$

where

$$c_{55}^{\text{eff}} = c_{55}^{\text{E}} \left(1 - \frac{e_{155}^{\text{E}}}{c_5^{\text{E}}} \bar{E}_1 \right) \quad (2.2.2\text{-}18)$$

$$e_{15}^{\text{eff}} = e_{15}\left(1 + \frac{M_{15}}{e_{15}}\bar{E}_1\right) \quad (2.2.2\text{-}19)$$

$$\varepsilon_{11}^{\text{eff}} = \varepsilon_{11}^{\text{S}}\left(1 + \frac{\varepsilon_{111}^{S}}{\varepsilon_{11}^{\text{S}}}\bar{E}_1\right) \quad (2.2.2\text{-}20)$$

Following similar procedure, we obtain the solution for impedance:

$$Z = j\omega\frac{w^{\text{eff}}l^{\text{eff}}}{t^{\text{eff}}\beta_{11}^{\text{eff}}}\left[1 - (k_{15}^{\text{eff}})^2\frac{\tan(\frac{kt^{\text{eff}}}{2})}{\frac{kt^{\text{eff}}}{2}}\right] \quad (2.2.2\text{-}21)$$

where w^{eff}, l^{eff}, t^{eff}, β_{11}^{eff} and k_{15}^{eff} are the corresponding effective width, length, thickness, permittivity and coupling factor of Y-cut CTGS crystal, respectively.

2.2.2.1 Nonlinear permittivity

As d_{11}, d_{12} and d_{13} of X-cut YCOB resonator all have nonzero values, its three-dimensional sizes will be converted to

$$t^{\text{eff}} = (1 + d_{11}\bar{E}_1)t \quad (2.2.2\text{-}22)$$

$$l^{\text{eff}} = (1 + d_{13}\bar{E}_1)l \quad (2.2.2\text{-}23)$$

$$w^{\text{eff}} = (1 + d_{12}\bar{E}_1)w \quad (2.2.2\text{-}24)$$

Thus, the effective dielectric constant of X-cut YCOB crystal can be calculated by

$$\beta_{11}^{\text{eff}} = \frac{w^{\text{eff}}l^{\text{eff}}}{C_0 t^{\text{eff}}} = \frac{w(1 + d_{12}\bar{E}_1)l(1 + d_{13}\bar{E}_1)}{C_0 t(1 + d_{11}\bar{E}_1)} \quad (2.2.2\text{-}25)$$

where C_0 is the capacitance at low frequency (1 kHz) and β_{11}^{eff} is the inverse of $\varepsilon_{11}^{\text{eff}}$:

$$\varepsilon_{11}^{\text{eff}} = \beta_{11}^{\text{eff}^{-1}} \quad (2.2.2\text{-}26)$$

It should be noticed that the effective permittivity measured here is in the clamped condition or under constant strain. According to Mason [18]'s results, two dielectric constants has following connection:

$$\frac{\varepsilon^T}{\varepsilon^S} = \frac{1}{1-k} \quad (2.2.2\text{-}27)$$

Then the nonlinear permittivity under constant strain is

$$\varepsilon_{111}^{\mathrm{S}} = \frac{\varepsilon_{11}^{\mathrm{eff}} - \varepsilon_{11}^{\mathrm{S}}}{\bar{E}_1} \quad (2.2.2\text{-}28)$$

In this case, the dimensions of X-cut YCOB resonator will be altered by a DC bias field. However, for other resonators in various orientations, the situation is quite different. For instance, the Y-cut CTGS resonator will not be affected as first three components in the second row of CTGS matrix of piezoelectric constants are all zero, which enables effective dielectric constant $\varepsilon_{22}^{\mathrm{eff}}$ to stay stable whatever the value of electric field is. According to Eq. (2.2.2-20), the nonlinear permittivity $\varepsilon_{222}^{\mathrm{S}}$ equals zero.

2.2.2.2 Nonlinear piezoelectric constant

The anti-resonance frequency has following denotation:

$$f_a = \frac{v}{2t^{\mathrm{eff}}} = \frac{1}{2t^{\mathrm{eff}}}\sqrt{\frac{c_{55}^D}{\rho}} \quad (2.2.2\text{-}29)$$

Considering the relationship between elastic compliance and stiffness that

$$c_{ij} = s_{ij}^{-1} \quad (2.2.2\text{-}30)$$

we could express elastic compliance under zero electric displacement as

$$s_{55}^{\mathrm{eff}} = \frac{1}{4\rho(t^{\mathrm{eff}} f_a)^2} \quad (2.2.2\text{-}31)$$

The ratio of two elastic constants under different boundary conditions is

$$\frac{\mathrm{s}^E}{s^D} = \frac{1}{1-k} \quad (2.2.2\text{-}32)$$

Then nonlinear piezoelectric constant could be gained by

$$e_{155}^{\mathrm{E}} = \frac{c_{55}^{\mathrm{eff}} - c_{55}^{\mathrm{E}}}{\bar{E}_1} \quad (2.2.2\text{-}33)$$

2.2.2.3 Electrostrictive constant

When $Z \to \infty$, coupling factor k_{15}^{eff} is written as

$$(k_{15}^{\mathrm{eff}})^2 = \frac{\frac{\pi}{2}\left(\frac{f_r}{f_a}\right)}{\tan\left[\frac{\pi}{2}\left(\frac{f_r}{f_a}\right)\right]} \quad (2.2.2\text{-}34)$$

while coupling factor k_{15}^{eff} is the ratio of three effective electromechanical coefficients:

$$(k_{15}^{\mathrm{eff}})^2 = \frac{\left(e_{15}^{\mathrm{eff}}\right)^2}{\varepsilon_{11}^{\mathrm{eff}} c_{55}^{\mathrm{eff}}} \quad (2.2.2\text{-}35)$$

Finally, dependent on the two equations above, piezoelectric constant e_{15}^{eff} could be derived:

$$\mathrm{M}_{15} = \frac{e_{15}^{\mathrm{eff}} - e_{15}}{\bar{E}_1} \quad (2.2.2\text{-}36)$$

which is the function to obtain nonlinear electrostrictive coefficient.

3.0 EXPERIMENTAL DESIGN

Since the approach to characterize nonlinear piezoelectric properties have already been extensively explained in last chapter, we could get started on the consideration of measurement process. The sample preparation and measurement system setup will be introduced in next section.

3.1 SAMPLE PROCESSIG

The whole procedure of crystal growth is so complicated that only a brief introduction upon growth condition of crystals is given in this article. Then it will be followed by an introduction about orientations of resonators that we choose with longitudinal vibration and thickness shear mode.

3.1.1 CTGS sample preparation

CTGS crystals whose chemical formula is $Ca_3TaGa_3Si_2O_4$ are outstanding among all other single crystals from langasite family because of its low cost for fabrication and promising electromechanical properties under high temperature.

Utilized solid state reaction, the compounds of four oxides: $CaCO_3$, Ta_2O_5, Ga_2O_3 and SiO_2 with extremely high purity have been fabricated under 1250℃ with desired ratio. The compounds are kept at this temperature for long enough time for the purpose of decomposition

carbon oxide of calcium. Afterwards, Czochralski approach is accepted to simulate the growth of CTGS single crystals from a CTGS bar in one direction, whose fundamental parameters are 0.5-1mm/h and 5-15rpm. The whole growing process is carried out under the atmosphere of Nitrogen and Oxygen at 1 vol% to prevent the reduction of gallium oxide. Finally, after all procedures mentioned above, we obtain the desired CTGS single crystals.

Considering various orientations of CTGS crystal, orthogonal coordinate axes are taken to denote different cuts of resonator in accordance with IEEE standard on Piezoelectricity [8]. The non-rotating crystal cuts could be expressed in two forms regarding their measurements. For the rectangular cuts featuring vibrations in longitudinal direction, first letter indicates thickness direction while the other one is along length direction. On the other hand, there is only one notation representing thickness orientation in square resonators.

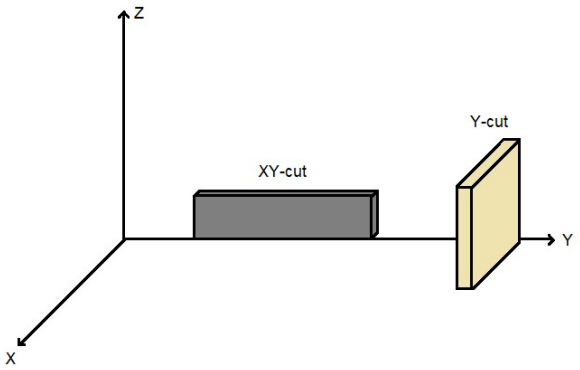

Figure 3. The orientations of CTGS resonators that we choose

Next, the deposition of electrodes on the top and bottom surfaces normal to thickness direction enables these insulated samples to receive electric signals. A sputtering system (ATC 1300-F) is used to deposit two layers of metal, chromium and gold with 50nm and 150 nm respectively.

3.1.2 YCOB sample preparation

Yttrium calcium oxyborate single crystal with chemical formula $YCa_4O(BO_3)_3$ has been chosen to investigate nonlinear properties as their potential abilities under high temperature as well. The YCOB samples are fabricated by three oxides ($CaCO_3$, Y_2O_3 and H_3BO_3) with similar method for CTGS crystals.

Regarding the matrices of linear permittivity, elastic coefficients as well as piezoelectric constants, totally six cuts (XY-cut, ZX-cut, ZY-cut, X-cut, Y-cut and Z-cut) whose orientations are described by coordinate axes following the principles from IEEE are qualified for the determination method that we illustrated above.

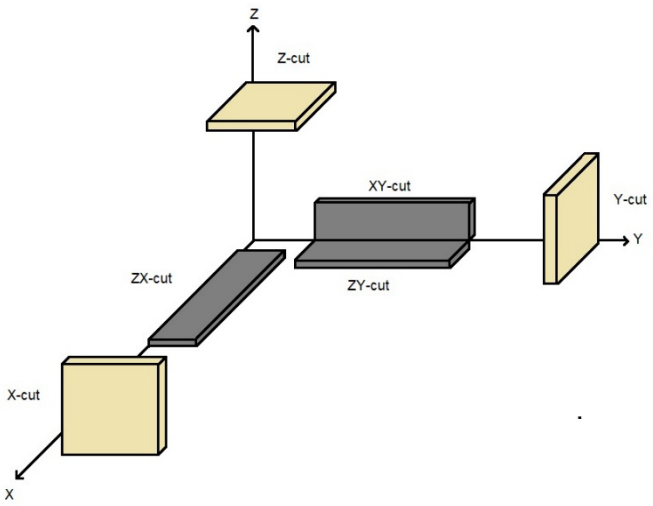

Figure 4. The orientation of YCOB resonators that we used

The electrodes on the desired surfaces of YCOB single crystals are deposited with the same method as CTGS samples which could be consulted in last section.

3.2 EXPERIMENTAL PREPARATION

The design of measurement system has been demonstrated in the schematic diagram below. A DC bias fixture (Agilent 16065) is utilized as a sample holder which accepts electric signals and exports output signals to be further analyzed. A DC voltage power (SRS PS325), the source of the DC bias fields, imports input in the range from -180v to +180v to the sample. Output signals affected by DC bias fields are received by an impedance analyzer (Agilent 4294A), then transformed to a data recording software (Labview) in the connected computer. The impedance analyzer makes it possible to capture the spectrums around resonance frequency and anti-resonance frequency as well as the values of capacitance at 1 kHz taken advantage to work out permittivity. The practical measurement system setup is shown in Figure 6.

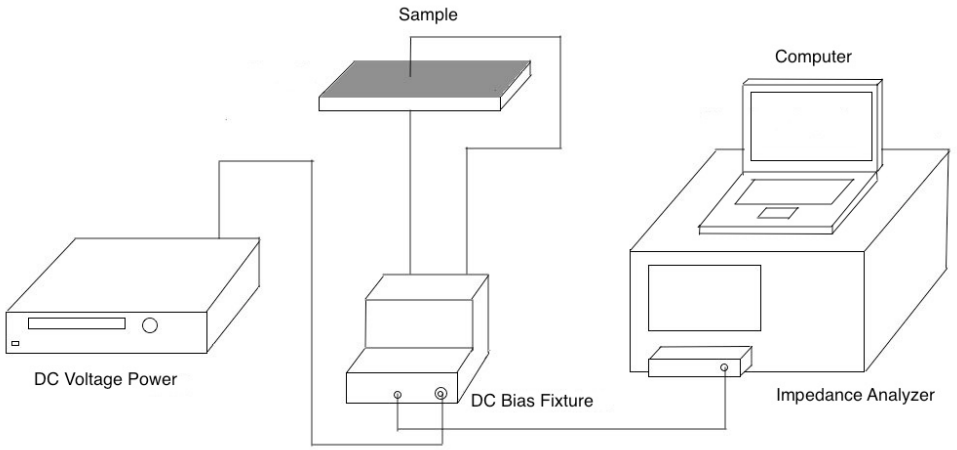

Figure 5. The schematic diagram of measurement system with DC bias field

Figure 6. The photograph of measurement system with DC bias field

4.0 RESULTS AND DISUSSION

Now that all experimental preparation is completed, the results could be computed following these steps. The first one is to measure resonance frequency and anti-resonance frequency under various DC bias fields. In the meantime, the capacitance at low frequency should also be obtained to figure out dielectric constants. Next, with the determination method for linear properties, we could work out the figures with variations of effective linear constants under different voltages. Last, the three nonlinear parameters are obtained by the slope shown in these figures.

It is noticed that, unlike the linear results obtained from PZT resonator [27], the variation of elastic and piezoelectric constants is always symmetric about zero electric field. This phenomenon could be explained by the difference in macroscopic structure between ceramics and crystals. For the typical isotropic ceramic resonator (PZT), its polarization won't be affected by external electric field. For crystals such as quartz, CTGS and YCOB, a DC bias field will cause the shifts of electric charges in molecules, then current will be produced by charge redistribution. The influence of positive and negative fields is the same because of identical surfaces of these piezoelectric crystals. However, the effective dielectric constants have a quite linear relationship with electric fields which could be illustrated by their independent of resonance frequency in calculation.

4.1 NONLINEARITY OF CTGS SINGLE CRYSTALS

For CTGS single crystals, there are only two efficient samples whose nonlinear properties could be measured with a DC bias field based on the matrices of linear coefficients. The results of resonators with different vibration mode will be discussed separately below.

4.1.1 Longitudinal vibration

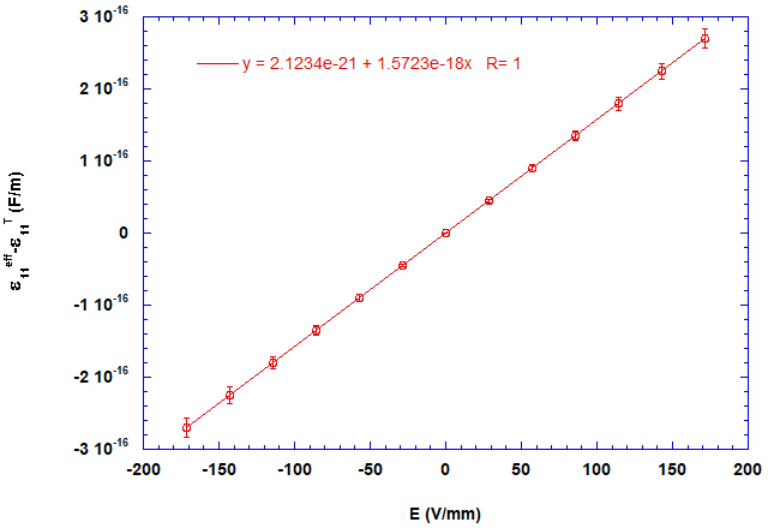

Figure 7. The variation of effective permittivity $\varepsilon_{11}^{\text{eff}}$ of CYGS single crystal with a DC bias field along X axis

In this identical mode of vibration, we could only successfully work out nonlinear parameters with XY-cut. It could be seen from Figure 7 that $\varepsilon_{11}^{\text{eff}}$ has excellent linear dependence on the electric field from -180V to +180V. After the linear regression, nonlinear permittivity (ε_{111}^{T}) could be deduced from the gradient. As observed in Figure 8, the effective elastic coefficients reduce as the absolute values of electric field increases which results in two negative values of d_{122}^{E} whose mean number is the approximate nonlinear piezoelectric coefficient for XY-cut.

Meanwhile, d_{12}^{eff} experiences the most variation as well as least linearity compared to other effective constants as electric field changes.

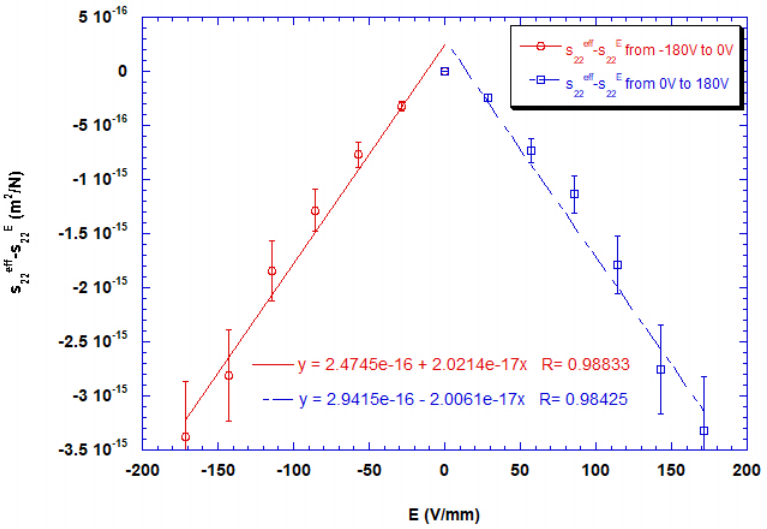

Figure 8. The variation of effective elastic compliance s_{22}^{eff} of CTGS single crystal with a DC bias field along X axis

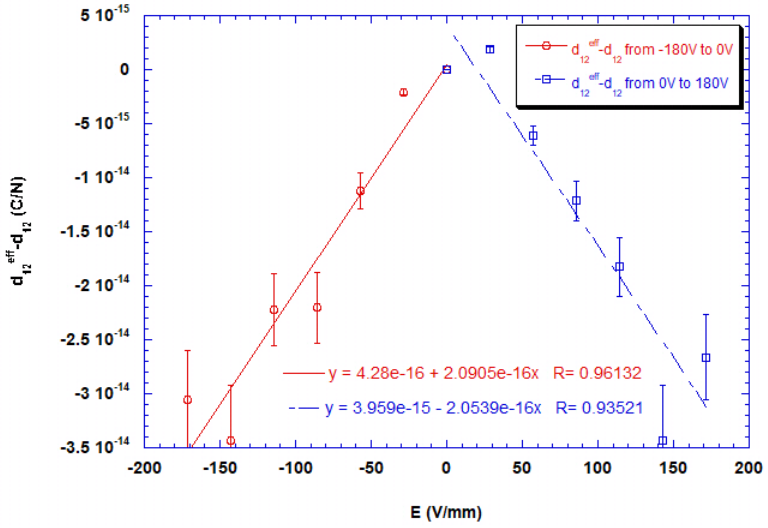

Figure 9. The variation of effective piezoelectric constants d_{12}^{eff} of CTGS single crystal with a DC bias field along X axis

4.1.2 Thickness shear vibration

The nonlinear dielectric constant of Y-cut CTGS resonator is zero as no deformation is caused by electric field in Y direction. Figure 10-11 give the variation of effective elastic stiffness and piezoelectric constant based on the same electric condition. It is discovered that c_{66}^{eff} is almost linear when external electric field grows while the distribution of e_{26}^{eff} processes less linearity. The measurement results of nonlinear coefficients, e_{266}^{E} and M_{26}, are positive and negative, respectively.

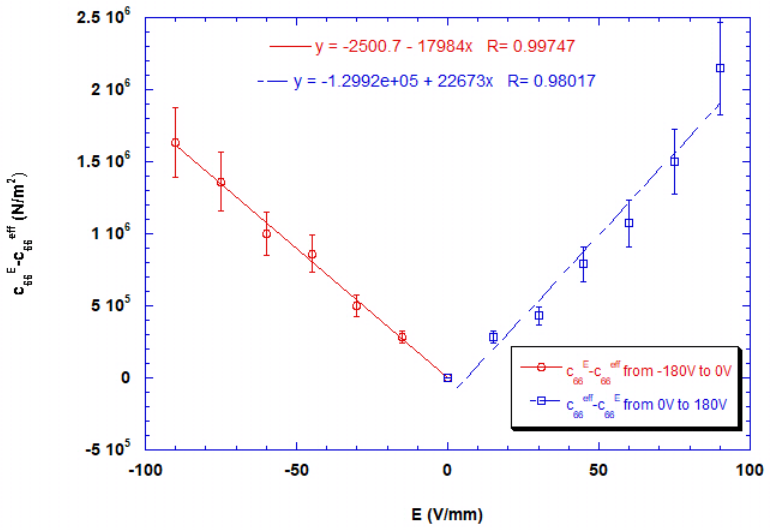

Figure 10. The variation of effective elastic stiffness c_{66}^{eff} of CTGS single crystal with a DC bias field along Y axis

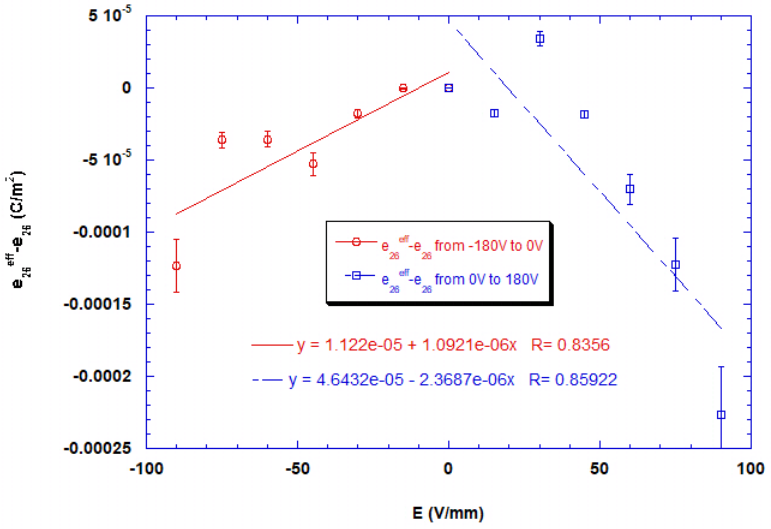

Figure 11. The variation of effective piezoelectric constants e_{26}^{eff} of CTGS single crystal with a DC bias field along Y axis

4.2 NONLINEARITY OF YCOB SINGLE CRYSTALS

Compared with CTGS single crystals, there are more nonlinear properties of YCOB single crystals available to be characterized. In this article, three square plates (XY-cut, ZX-cut and ZY-cut) as well as three rectangular plates (X-cut, Y-cut, and Z-cut) are considered.

4.2.1 Longitudinal vibration

Figure 12 exhibits the dielectric performance of XY-cut resonators under a DC bias field which is utilized in the deduction of ε_{111}^{T}. Another nonlinear dielectric property ε_{333}^{T} is characterized by the other two samples (ZX-cut and ZY-cut) in the condition of electric field in Y direction. It could be

summarized from the gradients in the figure 13-14 that YCOB single crystals have larger values of nonlinear permittivity along Z axis than that in X direction.

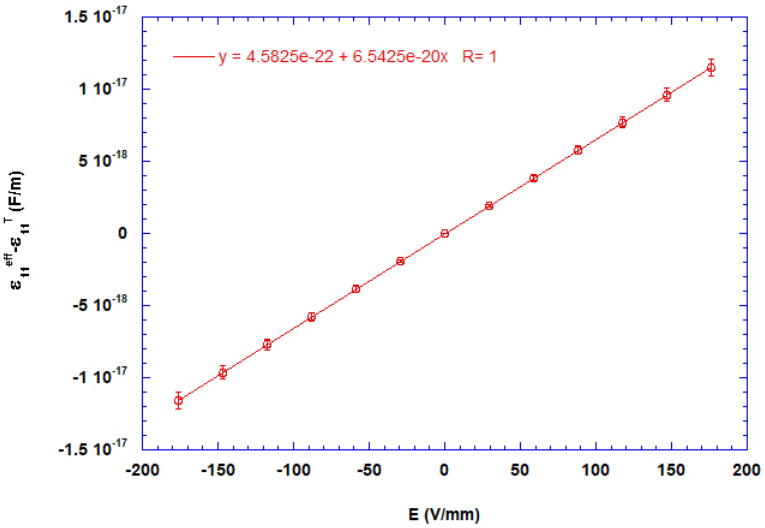

Figure 12. The variation of effective permittivity $\varepsilon_{11}^{\text{eff}}$ of YCOB single crystal with a DC bias field along X axis

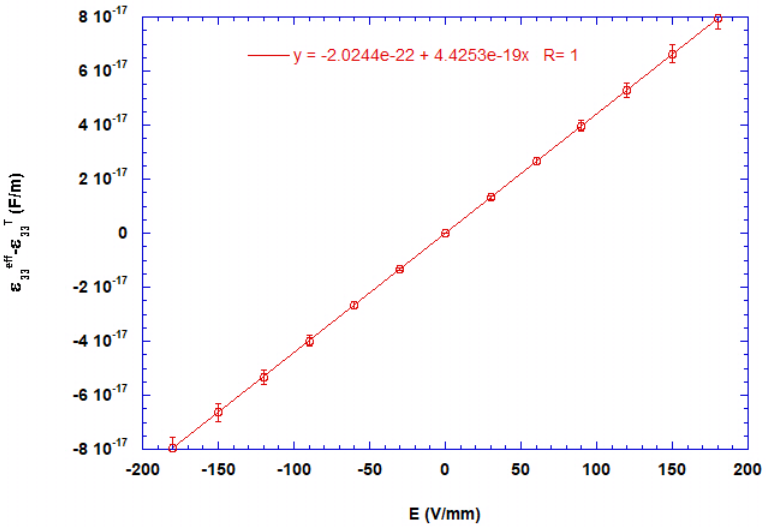

Figure 13. The variation of effective permittivity $\varepsilon_{33}^{\text{eff}}$ of YCOB single crystal (ZX-cut) with a DC bias field along Z axis

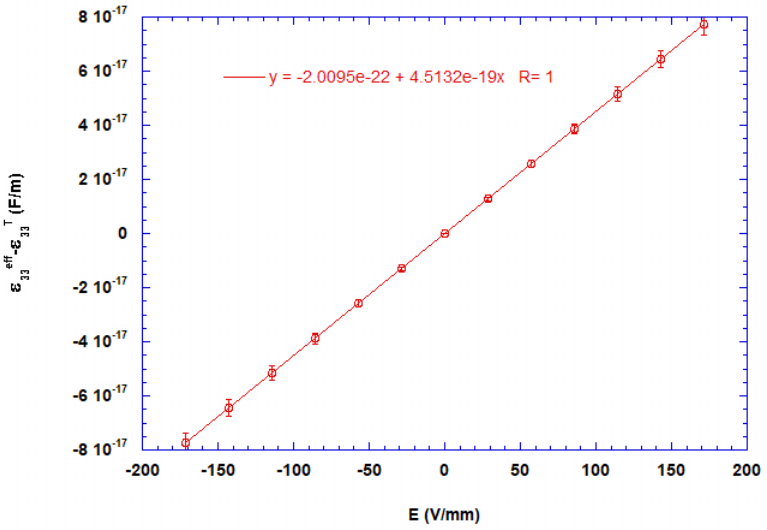

Figure 14. The variation of effective permittivity $\varepsilon_{33}^{\text{eff}}$ of YCOB single crystal (ZY-cut) with a DC bias field along Z axis

When external electric field goes up linearly, the variation of effective linear elastic compliances are shown in figure 15-17. All three third order piezoelectric constants (d_{122}^{E}, d_{311}^{E} and d_{322}^{E}) are found to be negative values. What's more, the differences between them are relatively small compare to other nonlinear electromechanical properties.

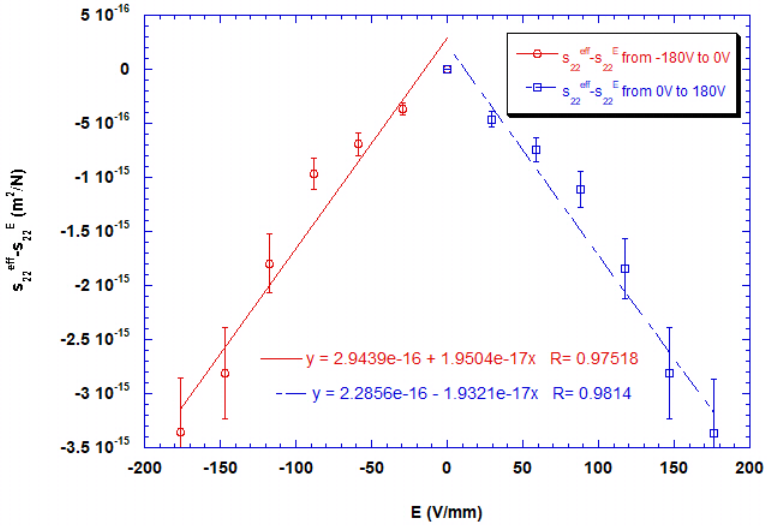

Figure 15. The variation of effective elastic compliance s_{22}^{eff} of YCOB single crystal with a DC bias field along X axis

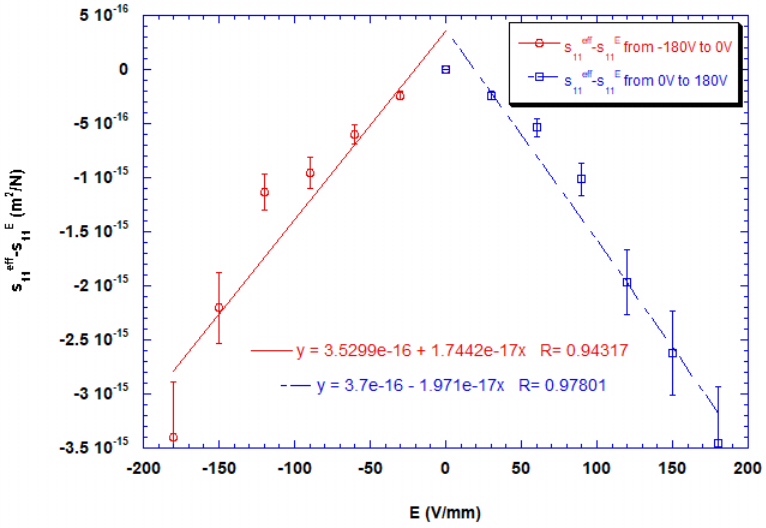

Figure 16. The variation of effective elastic compliance s_{11}^{eff} of YCOB single crystal with a DC bias field along Z axis

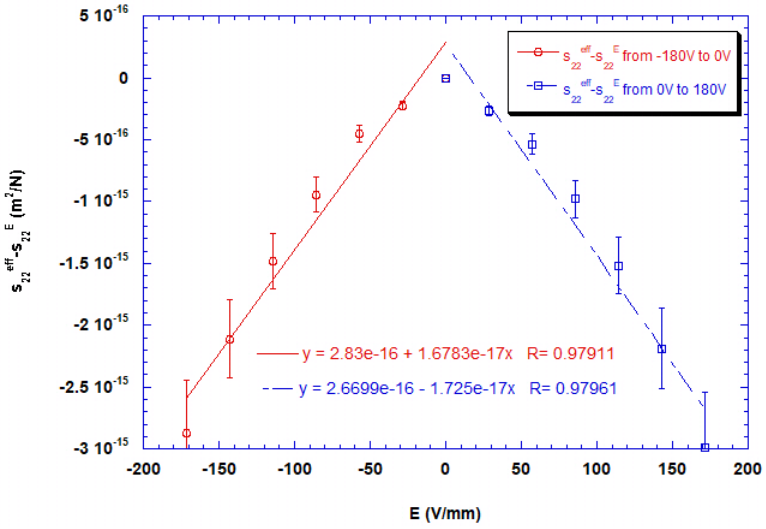

Figure 17. The variation of effective elastic compliance s_{22}^{eff} of YCOB single crystal with a DC bias field along Z axis

Three electrostrictive constants (M_{12}, M_{31} and M_{32}) are illustrated as the gradients in figure 18-20. Because of the formulas being used, electrostrictive properties seem to have the biggest errors after linear fitting is employed. In addition, M_{12} and M_{31} are both positive while M_{31} processes negative values.

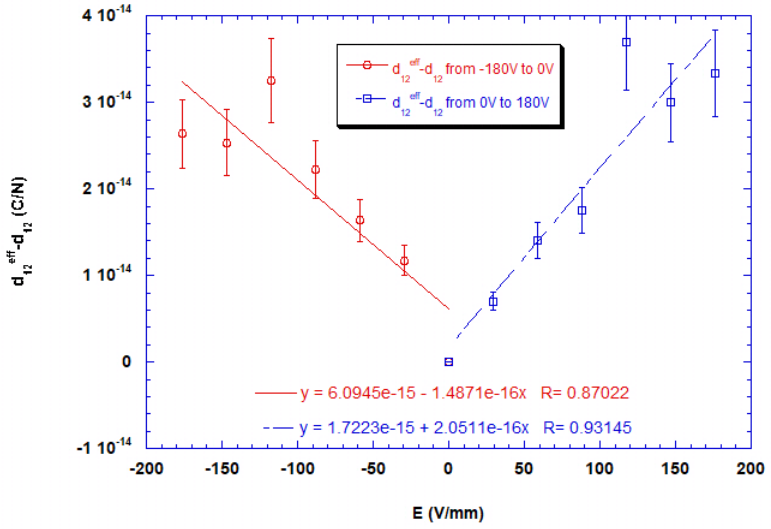

Figure 18. The variation of effective piezoelectric constants d_{12}^{eff} of YCOB single crystal with a DC bias field along X axis

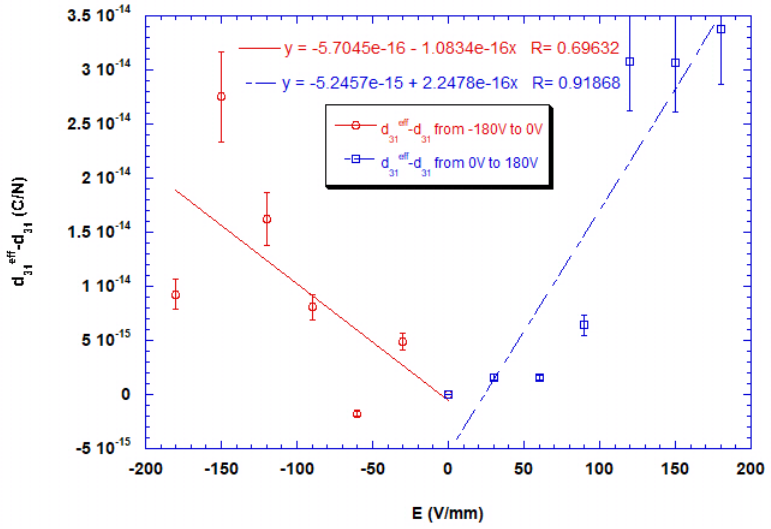

Figure 19. The variation of effective piezoelectric constants d_{31}^{eff} of YCOB single crystal with a DC bias field along Z axis

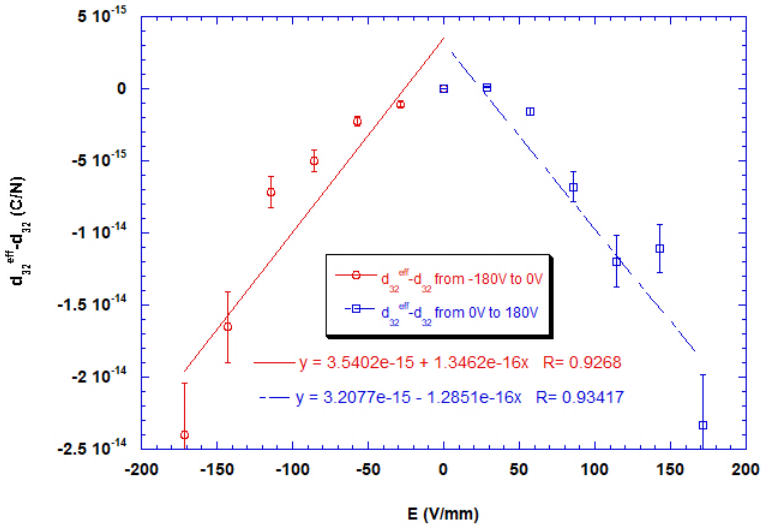

Figure 20. The variation of effective piezoelectric constants d_{32}^{eff} of YCOB single crystal with a DC bias field along Z axis

4.2.2 Thickness shear vibration

Figure 21-22 present the variation of nonlinear dielectric constants according to a linear electric field from -180V to+180V. The zero values of linear piezoelectric constants (d_{21}, $d_{22}$and d_{23}) account for the existence of zero nonlinear permittivity ε_{222}^{S}. For the other two constants (ε_{111}^{S} and ε_{333}^{S}), they exhibit almost the same nonlinear dielectric properties as their extremely similar linear permittivity.

It has been concluded from Figure 23-26 that e_{155}^{E}, e_{244}^{E}, and e_{266}^{E} are three positive third order piezoelectric coefficients who have much more larger values compared to the only negative parameter, e_{355}^{E}. All these results are calculated by the subtractive change of effective elastic stiffness.

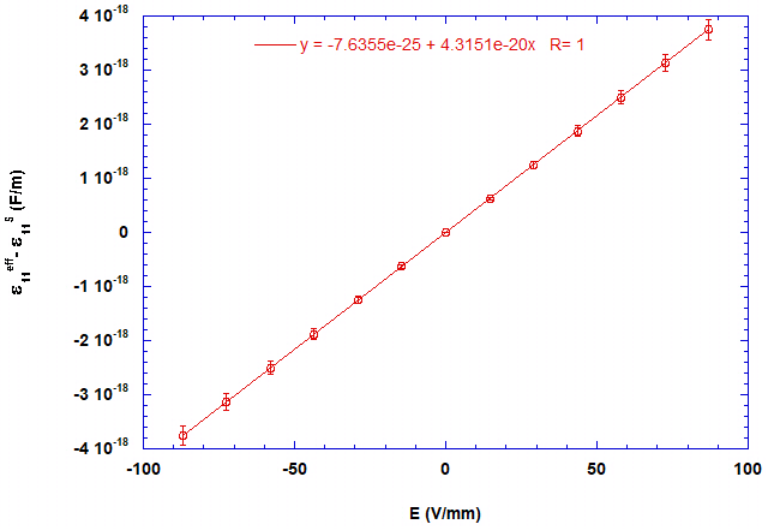

Figure 21. The variation of effective permittivity $\varepsilon_{11}^{\text{eff}}$ of YCOB single crystal with a DC bias field along X axis

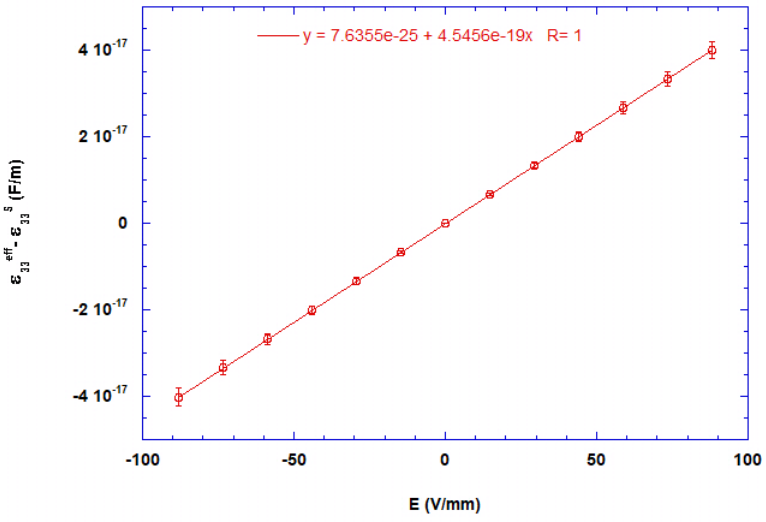

Figure 22. The variation of effective permittivity $\varepsilon_{33}^{\text{eff}}$ of YCOB single crystal with a DC bias field along Z axis

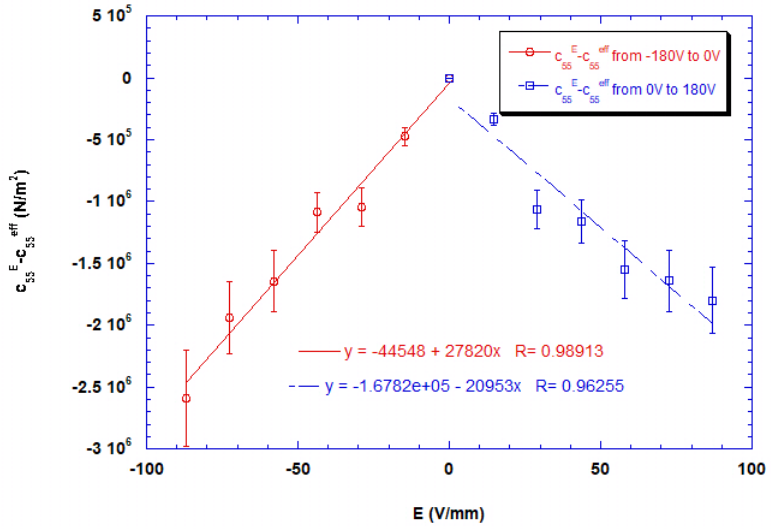

Figure 23. The variation of effective elastic stiffness c_{55}^{eff} of YCOB single crystal with a DC bias field along X axis

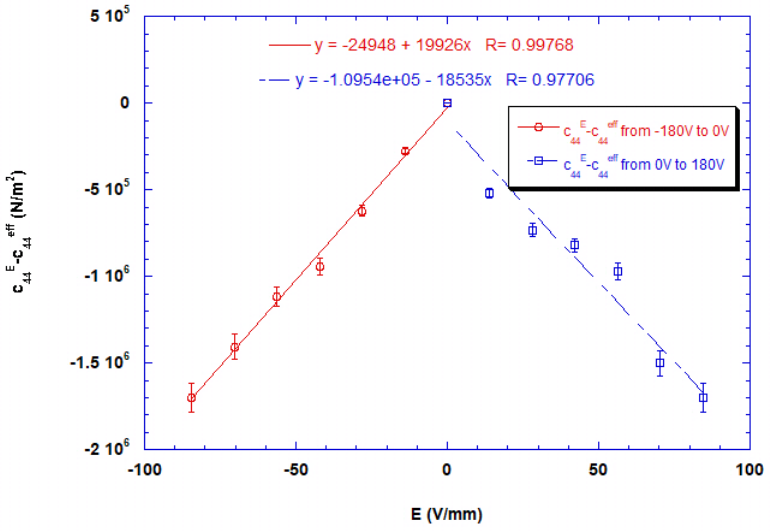

Figure 24. The variation of effective elastic stiffness c_{44}^{eff} of YCOB single crystal with a DC bias field along Y axis

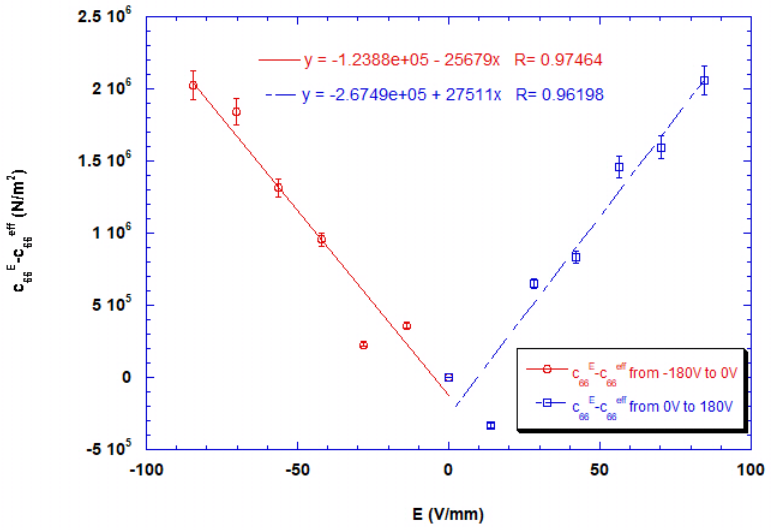

Figure 25. The variation of effective elastic stiffness c_{66}^{eff} of YCOB single crystal with a DC bias field along Y axis

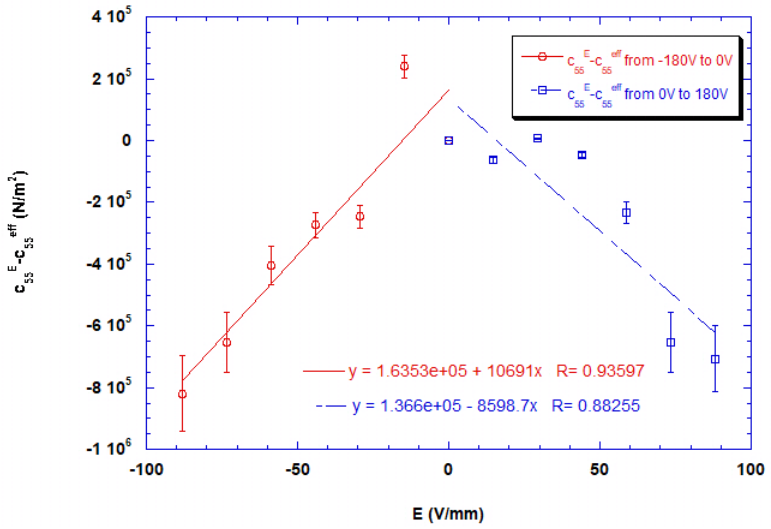

Figure 26. The variation of effective elastic stiffness c_{55}^{eff} of YCOB single crystal with a DC bias field along Z axis

Figure 27-30 show the behaviors of effective piezoelectric properties under the same DC bias field. All these four figures process poor linearity which could only be considered to characterize approximately electrostrictive results.

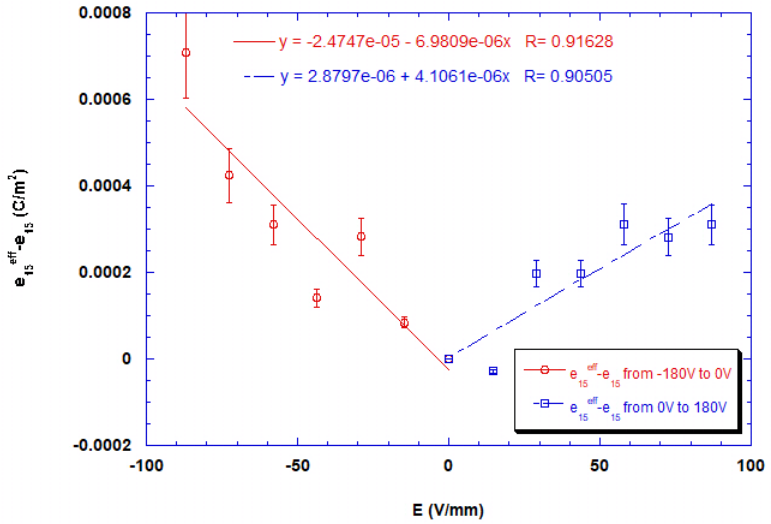

Figure 27. The variation of effective piezoelectric constants e_{15}^{eff} of YCOB single crystal with a DC bias field along X axis

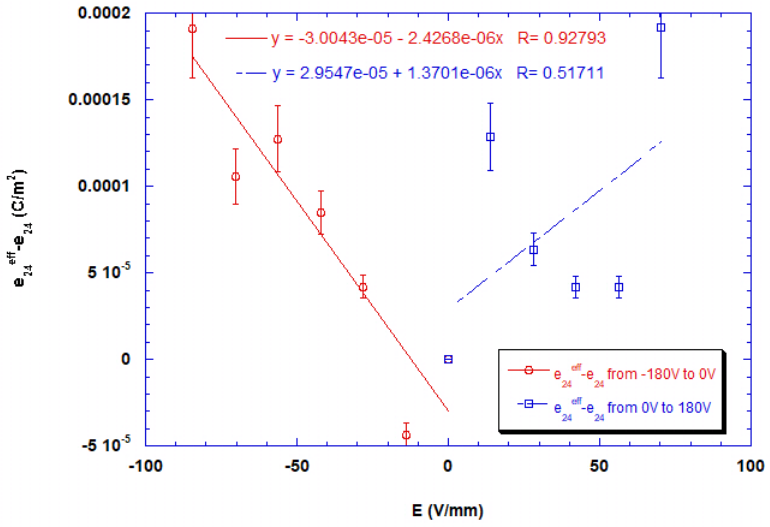

Figure 28. The variation of effective piezoelectric constants e_{24}^{eff} of YCOB single crystal with a DC bias field along Y axis

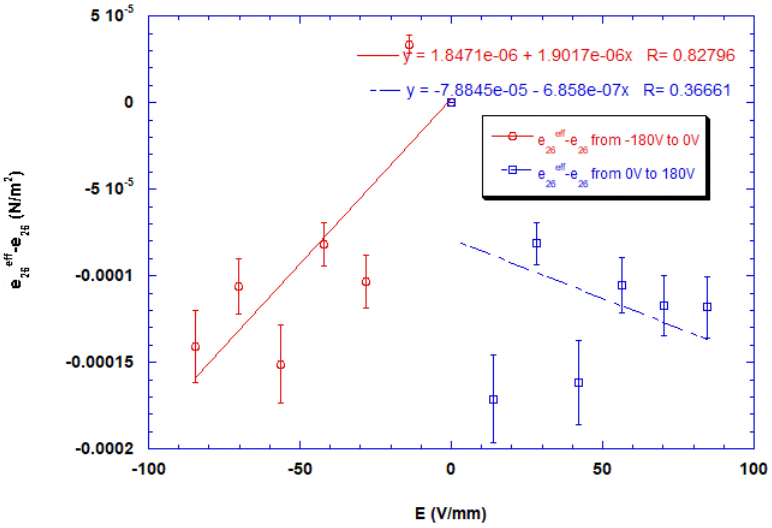

Figure 29. The variation of effective piezoelectric constants e_{26}^{eff} of YCOB single crystal with a DC bias field along Y axis

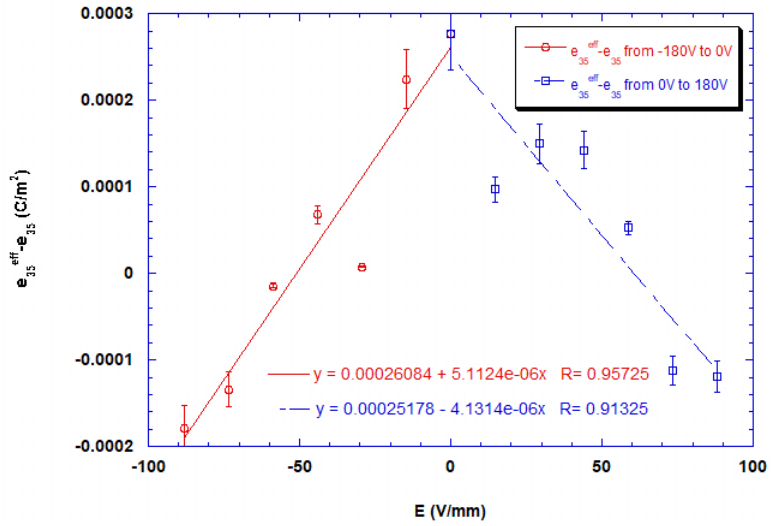

Figure 30. The variation of effective piezoelectric constants e_{35}^{eff} of YCOB single crystal with a DC bias field along Z axis

4.3 DISCUSSION AND CONCLUSION

Table 1. The summary of nonlinear coefficients of CTGS and YCOB single crystals measured under a DC bias field

Material	Nonlinear coefficients	Values		Mean values
		From -180V to0V	From 0V to +180V	
CTGS	ε_{111}^{T}	1.5723e-18	1.5723e-18	1.5723e-18
	ε_{222}^{S}	0	0	0
	d_{122}^{E}	-2.0214e-17	-2.0061e-17	2.1101e-17
	e_{266}^{E}	17984	22673	20328.5
	M_{12}	-2.0905e-16	-2.0539e-16	-2.0722e-16
	M_{26}	-1.0921e-06	-2.3687e-06	-1.7304e-06
YCOB	ε_{111}^{T}	6.5425e-20	6.5425e-20	6.5425e-20
	ε_{333}^{T}	4.4253e-19	4.4253e-19	4.4253e-19
		4.5132e-19	4.5132e-19	4.5132e-19
	ε_{111}^{S}	4.3151e-20	4.3151e-20	4.3151e-20
	ε_{222}^{S}	0	0	0
	ε_{333}^{S}	4.5456e-19	4.5456e-19	4.5456e-19
	d_{122}^{E}	-1.9504e-17	-1.9321e-17	-1.9413e-17
	d_{311}^{E}	-1.7442e-17	-1.9710e-17	-1.8576e-17
	d_{322}^{E}	-1.6783e-17	-1.7250e-17	-1.7017e-17
	e_{155}^{E}	-27820	-20953	-24386.5
	e_{244}^{E}	-19926	-18535	-19230.5
	e_{266}^{E}	25679	27511	26615
	e_{355}^{E}	-10691	-8589.7	9640.35
	M_{12}	1.4871e-16	2.0511e-16	1.7691e-16
	M_{31}	1.0834e-16	2.2478e-16	1.6656e-16
	M_{32}	-1.3462e-16	-1.2851e-16	-1.3157e-16
	M_{15}	6.9809e-06	4.1061e-06	5.5435e-06
	M_{24}	2.4268e-06	1.3701e-06	1.8985e-06
	M_{26}	-1.9017e-06	-6.858e-07	-1.2938e-06
	M_{35}	-5.1124e-06	-4.1314e-06	-4.6219e-06

a) The units of ε_{ijj}^{T}, ε_{ijj}^{S}, d_{jpq}^{E}, e_{jpq}^{E} are F/V, F/V, m^3/VN, N/mV, m^2/V^2.

b) The units of M_{12} and M_{26} of CTGS are m^2/V^2 and C/mV respectively.

c) The unit of M_{12}, M_{31} and M_{32} of YCOB is m^2/V^2 while the unit for other M_{jq} is C/mV.

All the values of nonlinear coefficients of CTGS and YCOB single crystals that we characterized by applying a DC bias field are summarized in Table 1. Among these three types of nonlinear coefficients, third order permittivity has the best accuracy while electrostrictive constants have

most errors based on the data we measured. What's more, from the good linearity between effective coefficients and external electric field shown in the experimental results, it has been proved that DC bias field could be effectively utilized as frequency compensators controlled by nonlinear coefficients.

5.0 BULK ACOUSTIC WAVE PRESSURE SENSOR

Apart from the DC bias field we adopted, external force is another efficient source. Its ability to simulate frequency shifts has also been proved. In this chapter, the measurement results of pressure-frequency sensitivity are represented, which provides the insights for the future development of pressure sensor.

5.1 FORCE-FREQUENCY EFFECT

When an external force is applied to a resonator, the shifts of resonance frequency will be caused by the related stress. This phenomenon is called force-frequency effect. In some situations, because of the extremely high requirement of precision, this effect in electric devices is totally undesirable. Nevertheless, people still developed some advantageous applications such as pressure sensors depending on the excellent linearity between force and resonance frequency [31, 32].

Ratajski [33] concluded following widely accepted formula to express the influential factors of force sensitivity coefficient K_f after checking all potential variables

$$K_f(\psi, \vartheta) = \frac{\Delta f}{f_0}\frac{1}{F}\frac{D}{f_0} \qquad (\mathbf{5.1}\text{-}1)$$

where ψ, ϑ, f_0, F and D are rotated angle along X axis, the angle of force along X axis, resonance frequency, external force and diameter, respectively. Even though this empirical equation has been

derived, there is still no definite understanding of force-frequency effect until Lee [25] deduced following formula to explain the variations of resonance frequency caused by external force:

$$\frac{\Delta f}{f_0} = S_{initial} + \frac{1}{2c_{66}}(c_{166}S_1 + c_{266}S_2 + c_{366}S_3 + c_{466}S_4) \qquad (\mathbf{5.1}\text{-}2)$$

His derivation is carried out on the rotated Y cut quartz resonator who is a finite body with initial stress. In this formula, S_1, S_2, S_3 and S_4 express the components of strain tensor while $S_{initial}$ is accepted to represent initial deformation in this resonator. Also, four third order elastic constants, c_{166}, c_{266}, c_{366} and c_{466}, are utilized to explain the frequency shifts caused by external force or pressure. Then, experimental results obtained by Lee [25] are proved to be compatible with the theoretical analysis. As a result, it could be summarized that third order elastic constants are responsible for force-frequency effects.

5.2 PREVIOUS WORK

In this section, Hongfei [30]'s investigations upon third order nonlinear elastic coefficients based on CTGS Y-cut resonator will be introduced. His work has been taken as the foundation of our research with bulk acoustic wave YCOB pressure sensor.

Based on the measurement system, Hongfei [30] derived following expression for CTGS bulk acoustic wave pressure sensor by replacing incremental strain components by linear elastic compliance and then transforming the external force by pressure:

$$\frac{\Delta f}{f_0} = \frac{\alpha}{A_2}\left[s_{11} + \frac{1}{2c_{66}}(c_{166}s_{11} + c_{266}s_{12} + c_{366}s_{13} + c_{466}s_{14})\right] \cdot \Delta P \qquad (5.2\text{-}1)$$

where c_{i66}, c_{66}, ΔP, Δf, A_2 and α are third order nonlinear elastic constants, linear elastic compliance, pressure difference, frequency shifts, depth of holder and the ratio of force to pressure difference which could be expressed as

$$\alpha = \frac{\pi r^4}{\frac{128\pi D h_1}{E_s A_1} + \frac{64\pi D h_2}{E_c A_2} + 4r^2} \quad (5.2\text{-}2)$$

Here, external force is assumed in X direction. Then, using similar way to define force sensitivity coefficient (K_f), he represented the pressure-frequency sensitivity (S_p) as

$$S_p = \frac{\Delta f}{f_0}\frac{1}{\Delta P} \quad (5.2\text{-}3)$$

Therefore, the final expression for pressure sensitivity for CTGS single crystals with pressure along X-axis is concluded as

$$S_p = \frac{\alpha}{A_2}\left[s_{11} + \frac{1}{2c_{66}}(c_{166}s_{11} + c_{266}s_{12} + c_{366}s_{13} + c_{466}s_{14})\right] \quad (5.2\text{-}4)$$

In the next step, Hongfei [30] measured the variation of resonance frequency over pressure difference from 0 to 45 PSI then the value of S_p could be calculated. Finally, the effective third order elastic coefficients s^*_{166} consisting of four third order elastic constants, could be obtained. By applying external pressure from Z direction of CTGS Y-cut resonator, he characterized another effective nonlinear coefficient s^*_{366}. Both coefficients clearly express the linear relationship of pressure and resonance frequency, which are the crucial parameters for CTGS single crystals to fabricate bulk acoustic wave pressure sensor.

5.3 YCOB PRESSURE SENSOR

In this section, based on the previous work, we choose X-cut and Z-cut YCOB resonators to measure their pressure sensitivities, which could be adopted to characterize the fundamental parameters for bulk acoustic wave pressure sensor.

5.3.1 Measurement system setup

The measurement system we adopt here is the same one in Hongfei [30]'s work. We took a pressure tubing with sample holders inside as the main part of measurement system. A nitrogen gas tank was connected to provide pressure from 0 to 40 PSI. The same impedance analyzer was used again to measure the shifts of resonance frequency. The pressure tubing that we utilize here is made of 304 stainless steel.

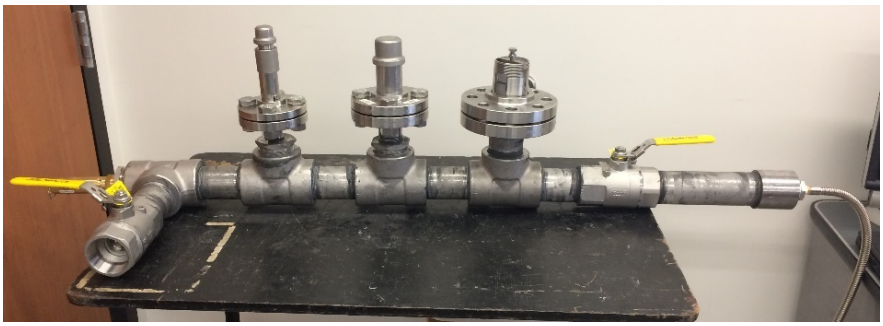

Figure 31. The photograph of pressure tubing

5.3.2 Results and conclusion

The sensitivity of YCOB pressure sensor that we used here could be illustrated by the formula:

$$S_p = \frac{\Delta f}{f_0}\frac{1}{\Delta P} \qquad (5.3.2\text{-}1)$$

where S_p, f_0 and ΔP are pressure sensitivity, resonance frequency and pressure difference respectively. The measurement results that we gained are shown in Figure 32-35 and Table 2.

From the behavior in the figures below, it could be discovered that both resonance frequencies of resonators present good linearity with pressure. In addition, compared to the pressure field from Z direction, X-cut sample is more sensitive to the pressure along Y axis. For Z-cut resonator, it processes similar sensitivity to pressure from both X and Y axes.

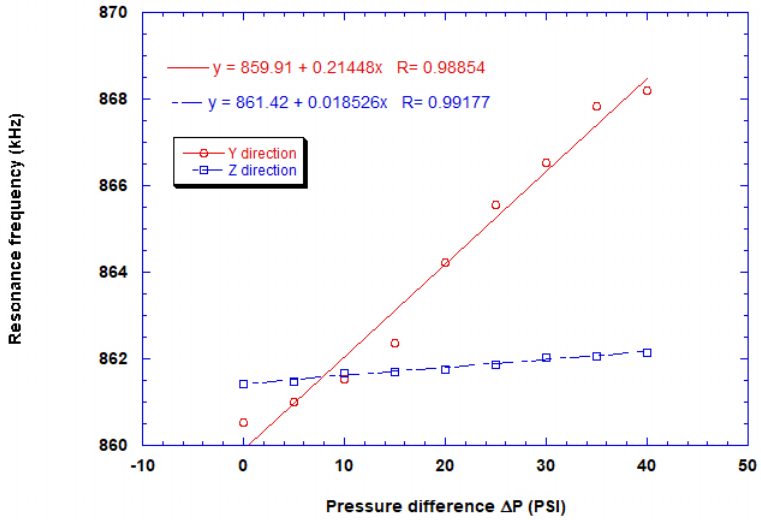

Figure 32. Resonance frequency of YCOB X-cut resonator when force is along Y and Z axis

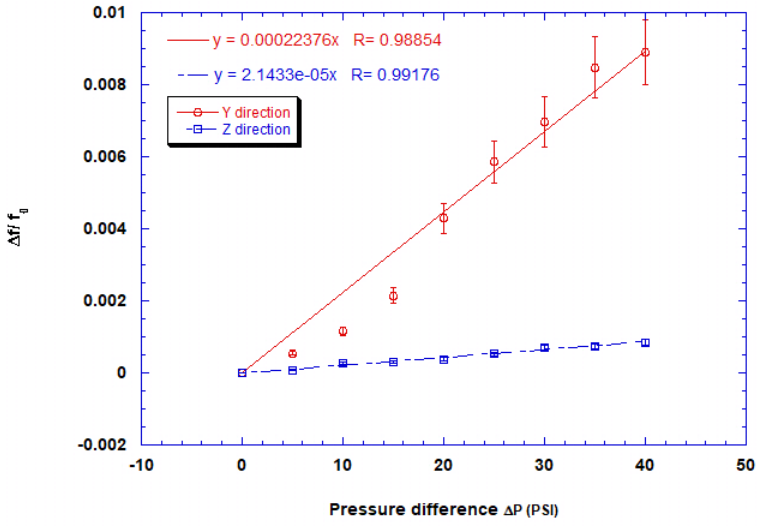

Figure 33. The variation of resonance frequency of YCOB X-cut resonator when force is along Y and Z axis

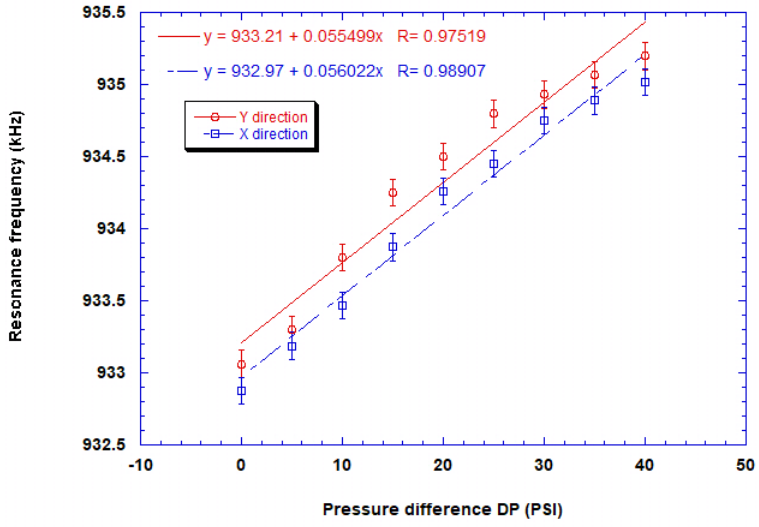

Figure 34. Resonance frequency of YCOB Z-cut resonator when force is along X and Y axis

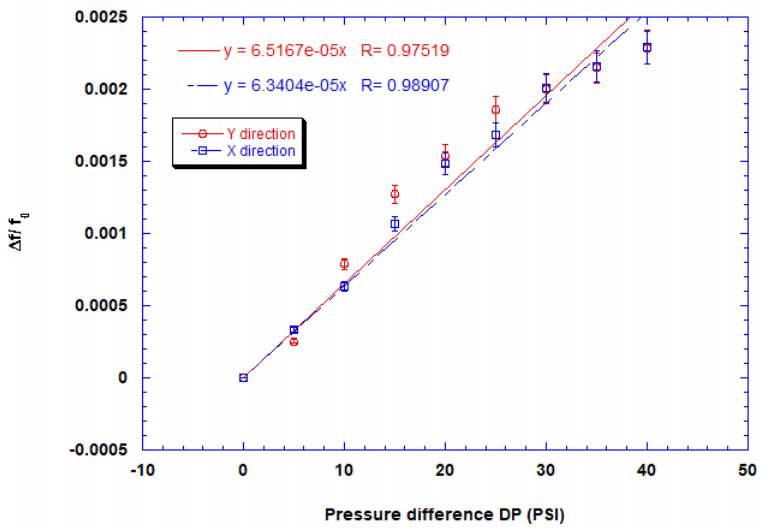

Figure 35. The variation of resonance frequency of YCOB Z-cut resonator when force is along X and Y axis

Table 2. The summary of pressure sensitivity of YCOB single crystals

The orientation of YCOB resonator	Force direction	Pressure sensitivity S_p
X-cut	Y	2.2376e-04
	Z	2.1433e-05
Z-cut	X	6.3404e-05
	Y	6.5167e-05

a) The units of S_p is in^2/lbf..

6.0 CONCLUSION REMARKS AND FUTURE WORK

In this article, third order piezoelectric constants, permittivity and electrostrictive coefficients of CTGS and YCOB crystals are investigated by introducing effective coefficients under a DC bias field from -180V to +180V. The determination process has been divided into thickness shear and longitudinal vibration according to the main vibration mode of resonators. From the measurement results, effective dielectric constants present the best linearity with the external electric field while effective elasticity comes next. Afterwards, with the application of YCOB bulk acoustic wave pressure sensors, it has been discovered that the largest value of pressure sensitivity occurs in the X-cut sample with pressure along Y direction.

For the future work, more samples with rotated cuts are suggested to be adopt in order to fully characterize all nonlinear electromechanical properties. What's more, the theoretical derivation of force-frequency sensitivity with third order elastic constants is worthy to figure out so that pressure sensors working in more precise environment could be designed and fabricated.

BIBLIOGRAPHY

[1] K. Aleksandrov, M. Zaitseva, A. Sysoev, and Y. I. Kokorin, "The piezoelectric resonator in a dc electric field," *Ferroelectrics*, vol. 41, no. 1, pp. 3-8, 1982.

[2] J. Curie and P. Curie, "Development by pressure of polar electricity in hemihedral crystals with inclined faces," *Bull. soc. min. de France,* vol. 3, p. 90, 1880.

[3] A. S. W. G. Hankel, 12, 547, 1881, vol. 12, p. 457, 1881.

[4] D. Ballantine Jr *et al.*, *Acoustic wave sensors: theory, design and physico-chemical applications*. Elsevier, 1996.

[5] P. Langevin and C. Chilowsky, "Echo sounding," *Hydrographic Review,* vol. 2, p. 75, 1924.

[6] G. Gautschi, "Piezoelectric sensors," in *Piezoelectric Sensorics*: Springer, 2002, pp. 73-91.

[7] W. Voigt, *Lehrbuch der kristallphysik (mit ausschluss der kristalloptik)*. Springer-Verlag, 2014.

[8] A. Meitzler, H. Tiersten, A. Warner, D. Berlincourt, G. Couqin, and F. Welsh III, "IEEE standard on piezoelectricity," ed: Society, 1988.

[9] P. Glover *et al.*, "α/β phase transition in quartz monitored using acoustic emissions," *Geophysical Journal International,* vol. 120, no. 3, pp. 775-782, 1995.

[10] H. Jaffe and D. Berlincourt, "Piezoelectric transducer materials," *Proceedings of the IEEE,* vol. 53, no. 10, pp. 1372-1386, 1965.

[11] S. Zhang and F. Yu, "Piezoelectric materials for high temperature sensors," *Journal of the American Ceramic Society,* vol. 94, no. 10, pp. 3153-3170, 2011.

[12] C. Shekhar Pandey and J. Schreuer, "Elastic and piezoelectric constants of tourmaline single crystals at non-ambient temperatures determined by resonant ultrasound spectroscopy," *Journal of Applied Physics,* vol. 111, no. 1, p. 013516, 2012.

[13] R.-U. Barz, J. Schneider, and P. Gille, "High-temperature phase transitions of gallium orthophosphate (GaPO4)," *Z. Kristallogr,* vol. 214, pp. 845-849, 1999.

[14] P. Krempl, G. Schleinzer, and W. Wallno, "Gallium phosphate, GaPO4: a new piezoelectric crystal material for high-temperature sensorics," *Sensors and Actuators A: Physical,* vol. 61, no. 1-3, pp. 361-363, 1997.

[15] J. Hornsteiner, E. Born, and E. Riha, "Langasite for high temperature surface acoustic wave applications," *physica status solidi (a),* vol. 163, no. 1, 1997.

[16] A. A. Vives, *Piezoelectric transducers and applications*. Springer Science & Business Media, 2008.

[17] J. Tichy, J. Erhart, and E. Kittinger, *Fundamentals of piezoelectric sensorics*. Springer, 2010.

[18] W. P. Mason and H. Baerwald, "Piezoelectric crystals and their applications to ultrasonics," *Physics Today,* vol. 4, p. 23, 1951.

[19] M. Vijaya, *Piezoelectric materials and devices: Applications in engineering and medical sciences*. CRC Press, 2012.

[20] J. Gagnepain and R. Besson, "Nonlinear effects in piezoelectric quartz crystals," in *Physical Acoustics,* vol. 11: Elsevier, 1975, pp. 245-288.

[21] S. P. Joshi, "Non-linear constitutive relations for piezoceramic materials," *Smart Materials and Structures,* vol. 1, no. 1, p. 80, 1992.

[22] J. Yang, *An introduction to the theory of piezoelectricity*. Springer Science & Business Media, 2004.

[23] S. Li, W. Cao, and L. Cross, "The extrinsic nature of nonlinear behavior observed in lead zirconate titanate ferroelectric ceramic," *Journal of applied physics,* vol. 69, no. 10, pp. 7219-7224, 1991.

[24] Q. Chen, T. Zhang, and Q.-M. Wang, "Frequency-temperature compensation of piezoelectric resonators by electric DC bias field," *IEEE transactions on ultrasonics, ferroelectrics, and frequency control,* vol. 52, no. 10, pp. 1627-1631, 2005.

[25] P. Lee, Y. Wang, and X. Markenscoff, "High− frequency vibrations of crystal plates under initial stresses," *The Journal of the Acoustical Society of America,* vol. 57, no. 1, pp. 95-105, 1975.

[26] W. Ren, S.-F. Liu, and B. K. Mukherjee, "Nonlinear behavior of piezoelectric lead zinc niobate–lead titanate single crystals under ac electric fields and dc bias," *Applied physics letters,* vol. 83, no. 25, pp. 5268-5270, 2003.

[27] Q.-M. Wang, T. Zhang, Q. Chen, and X.-H. Du, "Effect of DC bias field on the complex materials coefficients of piezoelectric resonators," *Sensors and Actuators A: Physical,* vol. 109, no. 1-2, pp. 149-155, 2003.

[28] D. Hall, "Review nonlinearity in piezoelectric ceramics," *Journal of materials science,* vol. 36, no. 19, pp. 4575-4601, 2001.

[29] X. Shi, D. Yuan, X. Yin, A. Wei, S. Guo, and F. Yu, "Crystal growth and dielectric, piezoelectric and elastic properties of Ca3TaGa3Si2O14 single crystal," *Solid State Communications,* vol. 142, no. 3, pp. 173-176, 2007.

[30] H. Zu, "High-Temperature Piezoelectric Bulk Acoustic Wave Sensors Based on Ca3TaGa3Si2O14 and YCa4O (BO3) 3 Single Crystals," University of Pittsburgh, 2017.

[31] H. Zhang, J. A. Turner, and J. A. Kosinski, "Experimental measurements of the force-frequency effect of thickness-mode langasite resonators," *IEEE transactions on ultrasonics, ferroelectrics, and frequency control,* vol. 60, no. 7, pp. 1475-1478, 2013.

[32] M. S. Patel and B. K. Sinha, "Force-frequency effect on the Q-factor of thickness-shear mode quartz and Langasite resonator at high temperatures," in *Ultrasonics Symposium (IUS), 2011 IEEE International*, 2011, pp. 316-319: IEEE.

[33] J. M. Ratajski, "The force sensitivity of AT-cut quartz crystals," in *20th Annual Symposium on Frequency Control. 1966*, 1966, pp. 33-49: IEEE.